



# Ocean cross-validated observations from the R/Vs L'Atalante, Maria S. Merian and Meteor and related platforms as part of the EUREC<sup>4</sup>A-OA/ATOMIC campaign

Pierre L'Hégaret<sup>1</sup>, Florian Schütte<sup>2</sup>, Sabrina Speich<sup>1</sup>, Gilles Reverdin<sup>3</sup>, Dariusz B. Baranowski<sup>4</sup>, Rena Czeschel<sup>5</sup>, Tim Fischer<sup>5</sup>, Gregory R. Foltz<sup>6</sup>, Karen J. Heywood<sup>7</sup>, Gerd Krahnemann<sup>5</sup>, Rémi Laxenaire<sup>1</sup>, Caroline Le Bihan<sup>8</sup>, Philippe Le Bot<sup>8</sup>, Stéphane Leizour<sup>8</sup>, Callum Rollo<sup>7</sup>, Michael Schlundt<sup>5</sup>, Elizabeth Siddle<sup>7</sup>, Corentin Subirade<sup>1</sup>, Dongxiao Zhang<sup>9,10</sup>, and Johannes Karstensen<sup>5</sup>

<sup>1</sup>LMD/IPSL, CNRS, ENS, École Polytechnique, Institut Polytechnique de Paris, PSL, Research University, Sorbonne Université, Paris, France

<sup>2</sup>Max-Planck-Institute for Meteorology, KlimaCampus, Hamburg, Germany

<sup>3</sup>Sorbonne Université, CNRS, IRD, MNHN, UMR7159 LOCEAN/IPSL, Paris, France

<sup>4</sup>Institute of Geophysics, Polish Academy of Sciences, Warsaw, Poland

<sup>5</sup>GEOMAR Helmholtz Centre for Ocean Research Kiel, Kiel, Germany

<sup>6</sup>NOAA, Atlantic Oceanographic and Meteorological Laboratory, Miami, FL, USA

<sup>7</sup>Centre for Ocean and Atmospheric Sciences, School of Environmental Sciences, University of East Anglia, Norwich, UK

<sup>8</sup>French Research Institute for Exploitation of the Sea (IFREMER), UBO, CNRS, IRD, Laboratoire d'Océanographie Physique et Spatiale (LOPS), IUEM, Plouzané, France

<sup>9</sup>Cooperative Institute for Climate, Ocean, and Ecosystem Studies, University of Washington, Seattle, WA, USA

<sup>10</sup>NOAA PMEL, Seattle, WA, USA

**Correspondence:** Pierre L'Hégaret (pierre.lhegaret@univ-brest.fr)

## Abstract.

The northwestern Tropical Atlantic Ocean is a turbulent region, filled with mesoscale eddies and large-scale currents. In this intense dynamical context, several water masses with thermohaline characteristics of different origins are advected, mixed, and stirred, at the surface and at depth. The EUREC<sup>4</sup>A-OA/ATOMIC experiment that took place in January and February 2020 was dedicated to assess the processes at play in this region, especially the interaction between the ocean and the atmosphere. For that, four oceanographic vessels and different autonomous platforms measured properties near the air-sea interface and acquired thousands of upper-ocean (400-2000 m) profiles. However, each device had its own observing capability, varying from deep measurements acquired during vessel stations to shipboard underway near-surface observations and measurements from autonomous and uncrewed systems (such as Saildrones). These observations were undertaken with a specific sampling strategy guided by near-real time satellite images and adapted every half day based on the process that was investigated. These processes were characterized by different spatio-temporal scales: from mesoscale eddies, with diameters exceeding 100 km, to submesoscale filaments of 1 km width. This article describes the data sets gathered from the different devices and how the data were calibrated and validated, in order to ensure an overall consistency, the platforms' datasets are cross-validated using a hierarchy of instruments defined by their own specificity and calibration procedures. This has enabled the quantification of the

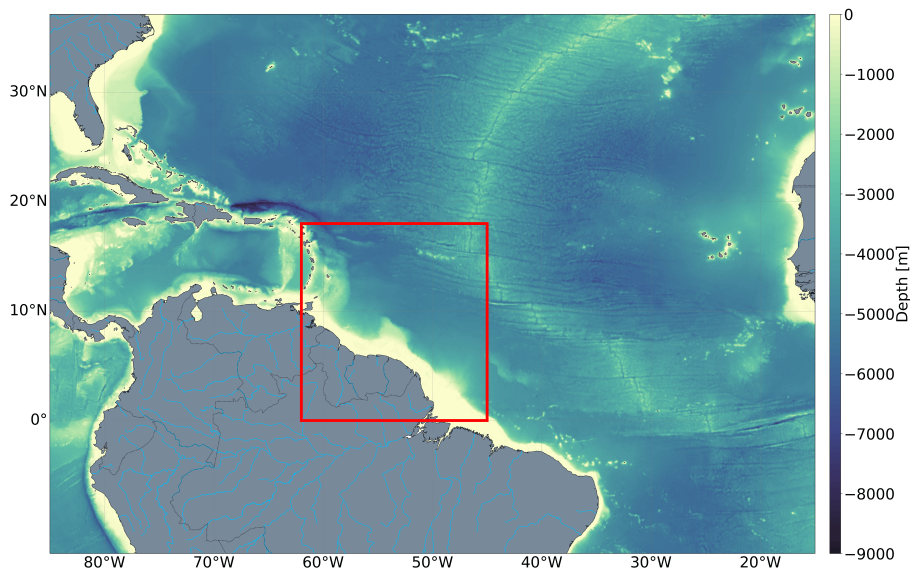


**Figure 1.** Bathymetric map of the northern tropical Atlantic Ocean, with the EUREC<sup>4</sup>A-OA/ATOMIC focus region framed in red.

15 uncertainty of the measured parameters when the different datasets are used together (<https://doi.org/10.17882/92071>).

## 1 Introduction

The international EUREC<sup>4</sup>A-ATOMIC initiative (<https://eurec4a-oa.eu/>) aimed to better understand the link between atmospheric shallow convection, cloud formation and the general circulation of the atmosphere (Stevens et al., 2021). The EUREC4A-OA experiment was embedded in EUREC4A-ATOMIC, and took place in January and February 2020 in the north-western Tropical Atlantic Ocean. EUREC<sup>4</sup>A-OA focused on the impact of meso- and submesoscale regional ocean dynamics on processes at the air-sea interface. The targeted ocean sampling for EUREC<sup>4</sup>A-OA was done with four research vessels: the German Maria S. Merian (Karstensen et al., 2020) and Meteor (Mohr et al., 2020), the French L'Atalante (Speich et al., 2021), and the US Ronald H. Brown (Quinn et al., 2021). In addition, various autonomous platforms (underwater electric gliders, surface drifters, Argo profiling floats, Saildrones and prototype drifting buoys OCARINA and PICCOLO (Bourras et al., 2014)) were operated in coordination with the ships.

The EUREC<sup>4</sup>A region (see Figure 1) can be divided into two subregions: one east of Barbados characterized by a rather stable wind-regime of easterlies ("Trade wind alley"), the other to the south and bounded by the South American continent, a region that hosts intense and long-lived northwestward-drifting mesoscale eddies spawned by North Brazil Current retroflexion ("Eddy boulevard"). Also, along the shelf break, the Amazon River plume flows northward and actively interacts with the

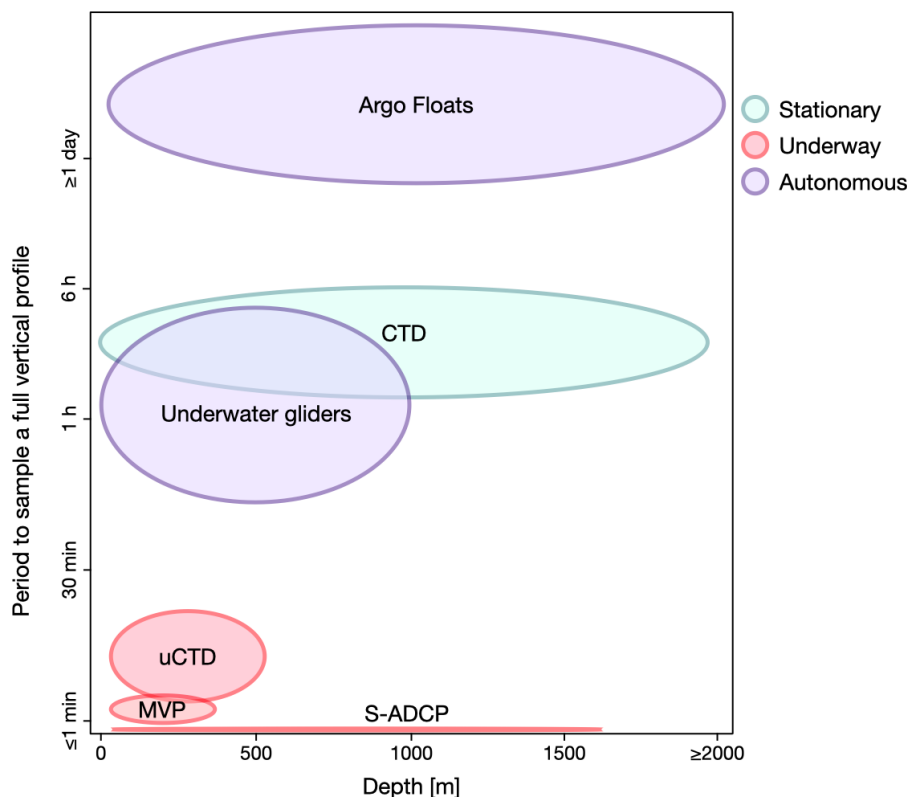


**Figure 2.** Schematic representation of the devices deployed during the EUREC<sup>4</sup>A-OA experiment, characterized by their frequency of acquisition for a full vertical profile and depth reached, considering the time of deployment. The green color indicates observations undertaken with the ship on station; the red color designates the devices acquiring data underway, whereas the purple color represents autonomous platforms.

North Brazil Current and its mesoscale eddies. In this dynamical context, several water masses of diverse origins are advected, stirred and mixed, preserving, however, large horizontal and vertical contrasts.

35 For observational studies of meso-/submesoscale features, some means of adaptive sampling is required. The EUREC<sup>4</sup>A-OA sampling was guided by analysis of near-real time satellite maps of Sea Surface Temperature, Sea Surface Salinity, altimetry (absolute dynamic height and related geostrophic velocities) and ocean color (Speich et al., 2021). Guided by the satellite information, the surveys were then done by various observational platforms in order to sample specific features, such as mesoscale eddies and fronts, freshwater pools, and filaments. To address the anticipated spatio-temporal sampling, the various platforms  
40 with different resolutions, autonomy, sensor payloads (Liblik et al., 2016), and periods required to acquire a profile, were used in a concerted effort (Figure 2). The sampling strategy was designed such that the phenomena would be measured with sufficient temporal and spatial resolution while also paying attention to the synchronicity of observations in the ocean and



atmosphere.

45 In order to ensure interoperable data for a parameter measured with various sensors, a comparative quality analysis was also performed, known as secondary quality control (QC). Secondary QC aims to create a coherent data set out of various data streams.

Gouretski and Jancke (2000) were among the first to present secondary quality control on oceanographic data through the use of "crossover analysis" in deep waters. This enabled them to conduct a rigorous QC assessment by comparing data from different sources and determine systematic errors such as Standard Seawater batch offsets. As for other similar studies (e.g., Tanhua et al. (2010)), a basic assumption is that deep water (typically >2000 m) properties are close to invariant. The need for QC methods in the upper layer received much attention through the global operations of profiling floats that typically are not recovered, and hence receive direct sensor QC only before deployment (e.g., in lab and in reference to standard or reference material). As introduced in for example Wong et al. (2003), by comparing with all nearby profile data and considering distance in space and time as a measure for impact, the offset, and drift behaviors of specific float measurements can be reconstructed.

The goal is to perform a quality assessment of a dataset, which in turn is composed of individual datasets from different observations platforms and sensors. For this purpose, we introduce here an assessment scheme of the individual datasets based on their traceability to reference data (traceability level). In the most optimal case, the reference material (RM) is a defacto standard (Otosaka et al., 2020), such as standard seawater for salinity, oxygen titration for dissolved oxygen, or triple point cells for temperature. As an example, for salinity the RM is Standard Seawater (SSW), giving a hierarchy as follows: SSW is assigned traceability level 0 and is used to reference a salinometer (Bacon et al., 2007) (traceability level 1). The salinometer readings for bottle samples are used as a statistical basis for the ship's CTD salinity correction (traceability level 2). The corrected ship CTD salinity is then further used to correct the TSG (traceability level 3). Bottle samples were also collected for the TSG and used via the salinometer as a statistical basis for the ship's CTD salinity correction (traceability level 2). The TSG is used to correct the MVP data (traceability level 4 or level 3, depending on the TSG calibration). Similar hierarchies can be built for all sensors.

Part of the Quality Assurance of the combined dataset is determining accuracy and precision, and also considering in this process the expected stability of the sensors given by the manufacturer. The CTD Rosette is key in the calibration process in respect of the secondary quality control. From the water samples collected with the Rosette sampler, numerous variables (in addition to conductivity, temperature, and pressure) are accessible throughout the water column, used for sensor calibration, laboratory analysis (e.g., oxygen titration), and to analyze biogeochemical parameters. However, its deployment requires the ship to remain on station for a few hours (depending on the attained depth) to perform the vertical profiles. The underway CTD (uCTD) and Moving Vessel Profiler (MVP) casts can be carried out underway, but they cannot dive deeper than about 450 m for the uCTD and about 200 m for the MVP model we employed (MVP30-300) (Branellec et al., 2020; Karstensen et al., 2020; Speich et al., 2021). Also, their sensors are more subject to bias than the CTD (Ullman and Hebert, 2014). Other devices, such



as underwater gliders, drifters, and Argo floats, are autonomous, but the data calibration is limited to certain times (deployment and recovery as shown on Figure 2) or by comparing sensor readings from nearby (time and space) data that has passed a QC.  
80 All the underway and autonomous devices rely on the proximity in space and time of CTD casts to validate and calibrate their measurements.

In the first part of this study, we present the calibration strategy we have adopted, as well as the hierarchy we defined between the sensors of each device. In the following sections, we present the instruments, providing information on when and where they were deployed, and how they were calibrated and validated. For parameters that have at least level 1 traceability,  
85 we estimate the uncertainty resulting from the cross-validation between platforms. Finally, we describe the final data set and the variables we provide for use to the scientific community.

## 2 Calibration strategy

90 The EUREC<sup>4</sup>A-OA experiment relied on numerous devices to measure physical and chemical properties of the water column from the three European ships and the various autonomous platforms deployed from the ships. We also include here the five US Saildrones funded under the NOAA and NASA ATOMIC project (Quinn et al., 2021; Gentemann et al., 2020). Their deployments were conducted by scientific staff originating from two institutions: GEOMAR (Kiel, Germany) and IFREMER (Brest, France). They have specific practices, sometimes leading to different procedures of deployment, data acquisition and calibration,  
95 tion, while still complying to international standards (Sloyan et al., 2019). The various calibration practices are either linked to similar devices from different manufacturers, or to various procedures in laboratories before and after the cruise. All the devices deployed during EUREC<sup>4</sup>A-OA are commonly used in oceanographic cruises, and the sources of errors and calibration procedures have been extensively documented and studied. In the next section, we briefly summarize them for each device.

100 At the top level of our hierarchy stands the most traceable sensors used to read water samples issued from the CTD bottles during every vertical profile or from the TSG circuit.

The CTD measurements are at the second level of the hierarchy, as its sensors went through careful pre-cruise and post-cruise calibration at the manufacturer's facility. Moreover, the sensor measurements are carefully validated and calibrated with samples collected and analyzed from the Rosette bottle water samples. CTD measurements serve as references for the calibration  
105 of all other observing platforms. Some TSG underway measurements also stand at traceability level 2 when calibrated with bottle samples.

Next in the ranking (traceability level 3) come those devices whose measurements are calibrated with the CTD, as they sample the same water (devices located on the same ship from which the CTD was deployed and measuring the same water as the CTD). These are the TSG when not directly calibrated with bottle samples, and the uCTD sensors when the probes were  
110 purposely mounted for calibration on the CTD rosette. The main sources of error here come from the method of deployment



of the devices and the sampling rate of the sensors.

Sensor data that only are calibrated via reference data close in space and time to the CTD profiles are labelled traceability level 4. The cross-calibration is then achieved by comparing the vertical profiles on T/S and depth/density diagrams. In this category fall most of the underway profiling devices: uCTD, MVP, and underwater gliders. As these measurements are not synchronous and not co-located with CTD profiles, an additional source of uncertainty arises from the spatio-temporal ocean variability. At the bottom of the hierarchy of traceability to a standard or an RM are the devices that cannot be compared directly either because their sensors are specific, measuring quantities that are not directly comparable with the CTD or that can be calibrated only by the manufacturers.

## 120 3 Ship observations

### 3.1 CTD rosette

On the R/Vs Maria S. Merian, Meteor, and L'Atalante a SeaBird SBE911+ CTD system was used for high-quality vertical profiling of the water column. Hereafter, we will describe briefly the calibrations and validations for each sensor. Other sensors were mounted to the CTD device (e.g., fluorescence, turbidity, particles) but are not considered here. Similar operational practices were carried out on all ships for CTD profiling. First, the CTD system was lowered to shallow depth ( 5 m) until the pump started. Then the CTD was brought back to the surface and subsequently lowered at approximately 0.5 m/s in the first 100 meters and 1 m/s for the deeper water column. The target depth varied, but in most cases reaching just above the seafloor. Water samples were collected with Niskin bottles mounted to the CTD rosettes. The samples were used for sensor calibration and for further analysis. The procedure for closing the bottles differed between the ships: on the R/V L'Atalante the CTD was stopped a few seconds for sampling, while on the R/V Maria S. Merian the samples were taken without stopping the CTD package.

In total the number of profiles acquired were 64, 86, and 266 for the R/Vs L'Atalante, Maria S. Merian and Meteor respectively (Figure 3).

135 The CTD rosettes on R/Vs Maria S. Merian and L'Atalante were also equipped with a Lowered Acoustic Doppler Current Profiler (L-ADCP) system composed, of an upward and a downward looking instrument, to record ocean current profiles.

#### 3.1.1 Pressure, Temperature, Conductivity, and Salinity quality assurance

Based on the manufacturer (SeaBird) specifications, the SBE9+ probe measures pressure with an initial accuracy of  $\pm 1.5 \cdot 10^{-2}\%$  and a resolution of  $\pm 1 \cdot 10^{-3}\%$  of the full scale of the respective CTD (6800 m for the R/Vs Maria S. Merian and

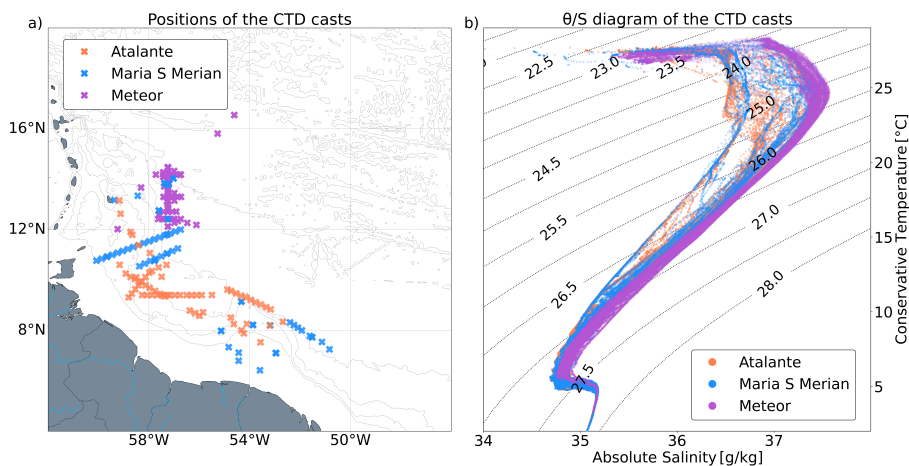


**Figure 3.** a) Map of the CTD casts positions for the R/Vs L'Atalante, Maria S. Merian and Meteor. b)  $\theta/S$  diagram of the CTD profiles for each ship superimposed on the isopycnals.

Meteor).

For the R/V L'Atalante, the pressure sensors are calibrated before and after the cruise at the IFREMER Laboratory of Metrology. The calibration is performed at a constant temperature of 20°C with increasing and decreasing pressure levels, with an uncertainty of 0.6dbar at 2000 meters depth. The bias, measured during the calibration, is then corrected by a polynomial of degree 4, associated with an uncertainty of  $\pm 0.12$ dbar. Good stability of the sensor was observed, with an overall uncertainty of  $\pm 0.72$ dbar. In addition, a validation was made using reversing pressure meter sensors (SIS RPM 6000X) at the bottom of the profiles and by comparing them with the CTD sensor to assess any drift. No drift were observed during the cruise, so after laboratory calibration and in-cruise validation, we assign the CTD pressure sensor level 2 traceability and an uncertainty on the order of the initial sensor accuracy of  $\pm 1.5 \cdot 10^{-2}\%$ . For the pressure sensors of the R/Vs Maria S. Merian and Meteor, no dedicated lab calibration was done before the cruise.

For all ships, the pressure sensor offset on deck before and after each profile was corrected in the processing as an offset, typically the mean of all values for each probe.

155

For each CTD, two SBE3+ temperature sensors from Seabird were mounted on the SBE911 probe, and the most stable sensor was used for the final calibration. The accuracy and resolution provided by the manufacturer are of  $\pm 1 \cdot 10^{-3}\text{°C}$  and  $\pm 2 \cdot 10^{-4}\text{°C}$ .

For the R/V L'Atalante, the temperature readings were calibrated at the IFREMER metrology lab before and after the cruise in reference to a Rosemount-type platinum resistance, periodically checked and certified, in a bath with strictly controlled temperature. The measurements were corrected by applying a polynomial of degree 3. The maximal error is lower than the

160



sensor accuracy provided by the manufacturer. In addition, the temperature sensor stability was monitored in comparison with two reversing thermometers (SIS RTM 4002X), one closed at the deepest depth of the profile, the other during the descent. No drift was observed during the cruise. For the R/Vs Maria S. Merian and Meteor, the sensors were calibrated before the cruise at an authorized lab.

For the temperature sensors from the CTD we thus assume an uncertainty of  $1 \cdot 10^{-3} \text{ }^\circ\text{C}$ , corresponding to the manufacturer accuracy, and we assign them level 2 traceability in our hierarchy.

Conductivity is measured with Seabird SBE4 sensors and, as for temperature, the most stable sensor is used for final calibration. In general, the procedures followed the GO-SHIP recommendations Hood et al. (2010), but details are provided below. The accuracy of the SBE4, as provided by the manufacturer, is  $\pm 3 \cdot 10^{-3} \text{ mS/cm}$  with a nominal stability of  $3 \cdot 10^{-4}$  per month and a resolution of  $\pm 4 \cdot 10^{-5} \text{ mS/cm}$  at 24Hz sampling.

For sensors used on the R/Vs, a lab calibration was done before the cruise by a manufacturer (Seabird) authorized laboratory. During the cruises, water samples were collected from Niskin bottles to perform a CTD conductivity calibration. Salinity of the water samples was analyzed on the R/V Maria S. Merian using an Optimare salinometer and on the R/V L'Atalante using a Portasal salinometer. The salinometers were in turn calibrated against a reference material, Standard Seawater. On the R/V Maria S. Merian a secondary reference also was used (labelled "substandard"), which is a large volume of water with unknown but constant salinity. At regular intervals, the substandard was measured with the salinometer and tracked for stability as an indicator of potential drift of the salinometer without the need to use large amounts of Standard Seawater. One other slight difference in procedures was the treatment of the water samples before analysis with the salinometer. In addition to adjusting the samples to the laboratory temperature (R/Vs Maria S. Merian and L'Atalante), the samples were degassed on the R/V Maria S. Merian. On earlier cruises, it was found that the Optimare salinometer is more sensitive to gas bubbles. For the purpose of degassing, the bottles were heated in a water bath to  $5\text{-}10^\circ\text{C}$  above laboratory temperature and then brought back to laboratory temperature. The released gas was extracted. Only then were the samples analyzed. More information on the CTDs and salinometers can be found in the cruise reports (Karstensen et al., 2020; Branellec et al., 2020). The salinity data from bottle samples of the R/Vs Maria S. Merian and L'Atalante is considered level 2 traceability.

The processing of CTD conductivity was done by first applying basic processing steps from the SBE processing routines (Seasoft V2) and including loop edit (0.2 m sec). The prepared raw data was then calibrated using the bottle sample analysis. Slightly different approaches were taken for the R/Vs Maria S. Merian and L'Atalante.

The R/V Meteor did not have a salinometer on board. Samples were taken for later analysis on shore, but the analysis could not be done. Some CTD profiles from the R/Vs Maria S. Merian and Meteor were performed close in space and time and covered the full water column. They are used here for the purpose of the R/V Meteor CTD salinity sensor calibration and





validation. Thus, the R/V Meteor salinity data is considered level 3 traceability.

For the R/V Maria S. Merian, the processing was as follows: after allocating a downcast profile segment to the upcast bottle sample stop via a vertical gradient criterion, the conductivity difference between bottle sample analysis and CTD sensor recording was calculated. The differences were sorted by magnitude, and the first 33% of all values were removed to eliminate outliers. Based on the remaining 66% of all values, correction equations were derived using pressure, conductivity, time, and sample number. Care was taken not to use high-order equations, as spurious interpolation may appear for weakly constrained segments of the multiparameter fit space. The uncertainty of the R/V Maria S. Merian sensors is estimated to be  $2 \cdot 10^{-3}$  psu, and the data are assigned level 2 traceability. A similar procedure was used for the oxygen sensor calibration based on the results from the Winckler titration.

For the R/V L'Atalante a set of three corrections was applied to remove large differences between the conductivity values of the sensor and water sample. First, a correction as a function of time was implemented to take into account a potential slow drift of the conductivity sensor. Second, a correction relative to the conductivity was applied. At each iteration of this correction, the samples showing  $\Delta C > 2.8 \times \sigma$ ,  $\Delta C$  being the difference between the sensor and the water sample conductivity, and  $\sigma$  the standard deviation of all the samples considered at each iteration, were removed. Third, a correction as a function of pressure was applied to the conductivity or salinity. After calibration of all casts, the standard deviation between the sensor data and the chemical data was  $2.3 \cdot 10^{-3}$  mS/cm for conductivity and  $2.3 \cdot 10^{-3}$  psu for salinity, both below the accuracies provided by Seabird. The uncertainty of the R/V L'Atalante sensors is thus of  $3 \cdot 10^{-3}$  psu, and they are considered level 2 traceability.

215

### 3.1.2 Dissolved Oxygen

Two SBE43 dissolved oxygen sensors were used for a range of measurements from 0 to 120% of the surface saturation. The accuracy from the manufacturer is 2% of the saturation. The sensor showing the more stable measurements was kept for data reduction.

Pre- and post-cruise lab calibrations were carried out on the sensors in laboratories in the same way as the temperature and conductivity sensors. As for conductivity, water samples were collected in bottles for calibration of the sensor measurements. The dissolved oxygen concentrations in the water samples were estimated using Winkler titration (Winkler, 1888). The chemistry reports for the different R/Vs describe the operating modes for the R/V L'Atalante (Branellec et al., 2020) and R/V Maria S. Merian (Karstensen et al., 2020).

After calibrations, the uncertainties of the oxygen measurements are  $1.60 \mu\text{mol/kg}$  for the R/V L'Atalante and  $0.61 \mu\text{mol/kg}$  for the R/V Maria S. Merian. The CTD oxygen data are considered level 2 traceability.



### 3.1.3 Lowered ADCP (L-ADCP)

For every CTD station on each ship, two Workhorse 300 kHz ADCP were attached to the CTD rosette with a Master-Slave configuration, one looking upward (Slave) and the other looking downward (Master). They provide current profiles from the surface to the maximum depth of the CTD cast. Reference velocities to derive velocity profiles from the velocity shear observations of the L-ADCP system were obtained from the ship ADCP (S-ADCP) and the bottom track (if available) following Thurnherr et al. (2010) and Sloyan et al. (2019). The accuracy of L-ADCP velocity measurements is estimated to be  $\pm 0.5$  cm/s. The velocity measurements are specific in our hierarchy of calibrations, since they can only be calibrated with cross-validation between devices and not with water samples. Therefore, we rank them level 2 traceability in the hierarchy of sensor/platform quality assurance.

### 3.1.4 Nutrients and Bio-optical measurements

While the previous sensors and procedures are similar for all three vessels, this is not the case for the measurement of nutrients and other biogeochemical properties.

The CTD rosette onboard the R/V Maria S. Merian was equipped with an OPUS UV spectral sensor for nitrate and carbon bond measurements, more specifically nitrate (NO<sub>3</sub>-N), nitrite (NO<sub>2</sub>-N) and numerous organic ingredients with a resolution of 0.8 nm/pixel using wavelengths of 200-360 nm. In addition, on all three ships, nutrients were analyzed from the bottle samples taken. On the R/V L'Atalante for each CTD cast, three bottles collected samples at different depths to measure Phosphate, Silicate, Nitrate, and Nitrite concentrations after the cruise. For the R/Vs Meteor and Maria S. Merian, these quantities, as well as ammonium, were measured on specific stations and at fixed depths between the surface and 350 meters.

Following the recommendation from GO-SHIP (Sloyan et al., 2019), numerous bio-optical sensors were also mounted on all CTD rosettes. The various sensors had very different and sometimes unknown lab or manufacturer calibrations. They are considered level -9, the lowest in our calibration hierarchy.

Chlorophyll fluorescence was measured via fluorometers. The CTD deployed from the R/V L'Atalante was equipped with a Chelsea AquaTracka III. The accuracy provided by the manufacturer is  $\pm 0.02$   $\mu\text{g/L}$  and its sensitivity is  $0.01$   $\mu\text{g/L}$ . The R/Vs Meteor and Maria S. Merian used Wet Labs Eco-AFL/FL fluorometers. Their sensitivity is  $0.025$   $\mu\text{g/L}$ . The CTD rosettes of the two German ships were also equipped with WET Labs Eco CDOM fluorometers, measuring the dissolved organic matter with a sensitivity of  $0.093$  ppb.

The CTD deployed from the R/V L'Atalante was instrumented with a C-Star transmissometer from Wet Labs, measuring particle beam attenuation coefficient.

The CTDs of the R/Vs Maria S. Merian and Meteor were also equipped with turbidity meters (WET Labs, Eco-NTU) to measure the turbidity of water with a sensitivity of  $0.02$  NTU (Nephelometric Turbidity Units) in the upper 125 meters of the water



column, and 0.12 NTU down to 1000 meters depth.

Finally, all three ships CTDs were equipped with PAR/Irradiance, Biospherical/Licor from Chelsea. This sensor measures the number of photons in the 400–700 nm wavelength, the spectral range of Photosynthetically Active Radiation (PAR), converted in  $\text{mMol/s/m}^2$ . Additionally, surface PAR/Irradiance sensors were mounted on both the R/Vs L'Atalante and Meteor CTD  
265 rosettes.

As these measurements were not validated, we did not add them to our hierarchy, nor did we perform a secondary calibration between devices.

### 3.2 Intercalibration of CTD data – the effect of oceanic variability

270 For all three ships, the acquisition of temperature, salinity, and dissolved oxygen data are performed with sensors that have similar accuracy and resolution. The calibration and validation of these quantities, performed by either IFREMER or GEOMAR, are in agreement with international recommendations from GO-SHIP. There are two main differences between the methodologies of deployment: for IFREMER, the first measurements started at a depth of 5 meters, while for GEOMAR they started at around 1.5 meters. For IFREMER, the upward movement of the CTD package was stopped for 30 seconds before closing the  
275 Niskin bottles, while for GEOMAR they were closed underway. To assess any discrepancies, a calibration of the raw measurements from the R/V L'Atalante CTD were performed with the GEOMAR procedures. Again, there are two notable differences in terms of calibration: First, the positioning of the CTD station was different between the methods. Second, the GEOMAR toolbox calibrates all the profiles together, while it was chosen to use the IFREMER toolbox to perform piecewise calibration on 5 to 6 profiles at a time. Excluding the interpolated surface layer, these different approaches showed no major differences  
280 in terms of temperature and salinity. For dissolved oxygen, the different calibration procedures can lead to differences of up  $5\mu\text{mol/kg}$ .

In general, at each isopycnal level, the differences between two profiles with small temporal and spatial separations can be linked to two sources: different calibration procedure and the internal ocean variability. As the IFREMER and GEOMAR  
285 CTDs calibration procedures provide similar if not equal results, the remaining differences between the various datasets must be due primarily to ocean variability. Figure 4a) and b) present the absolute salinity differences on isopycnal level, for each R/V, for CTD profiles found within a specific distance and time, respectively. As observed here, the averaged salinity differences, and associated standard deviation, depend on density. The largest variations are particularly displayed for the lighter density, close to the surface, and on isopycnal levels where large mesoscale eddies, the North Brazil Current rings, are known  
290 to evolve (Fratantoni et al., 1995). Moreover, these differences increase with time and distance (see Figure 4c) and d) for the vertically averaged absolute salinity differences), independently of the area of deployment. The R/V L'Atalante displays higher variability compared to the R/Vs Maria S. Merian and Meteor.

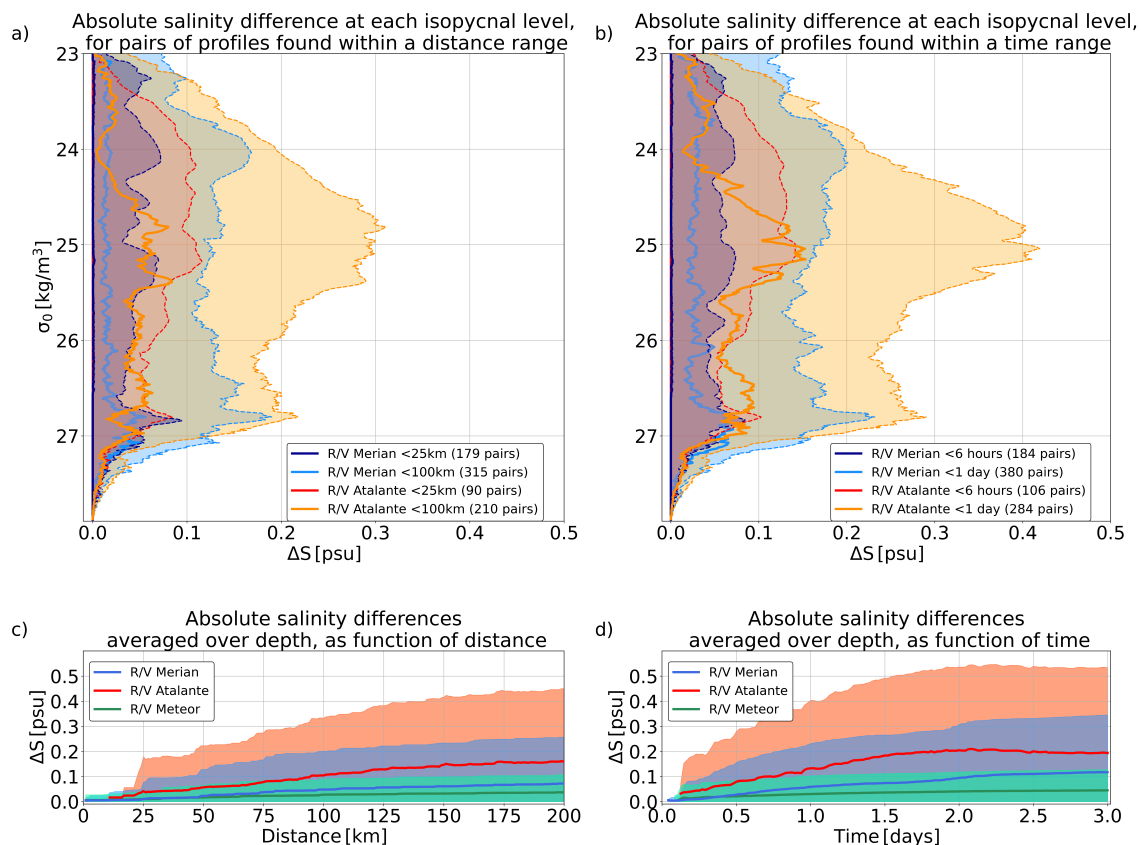


**Figure 4.** a) Absolute salinity difference between CTD pairs of profiles calculated on isopycnal levels for each R/V, averaged by distance. The dark blue and red curves are the average differences for profiles that are separated by less than 25 km for the R/Vs Maria S. Merian and L'Atalante respectively, while the blue and orange curves are for profiles found within 100 km. The shaded areas represented the standard deviation at each isopycnal level. b) Same as a) but with profiles averaged by time. The dark blue and red curves are for profiles separated by less than 6 hours, while the blue and orange are found within the same day, again for the R/Vs Maria S. Merian and L'Atalante respectively. c) Absolute salinity differences averaged vertically over the isopycnal levels as a function of distance for the R/Vs Maria S/ Merian (blue), L'Atalante (red), and Meteor (green). D) Same as c) but as a function of time instead of distance.

The calibrated CTD dataset for each R/V is associated to an uncertainty for every parameter. However, the creation of an assembled dataset gathering all profiles requires a comparison of these arrays. Figure 5 displays the vertically averaged differences for each parameter, removing the first 50 m to avoid taking into account the surface oceanic variability. The left column shows these differences for profiles performed by the same R/V as a function of both time and distance, also represented by the blue and red curves on the right panels. These curves exhibit the oceanic variability plus the post-calibration uncertainty; for near-by CTD pairs, they tend towards this last value. The central column of Figure 5 represents the difference calculated with one CTD profiles from each R/V, synthesized by the green curves on the right panels. This curve is the result of both oceanic variability and uncertainty linked to the differences of deployment and calibration between each R/V and laboratory. For all

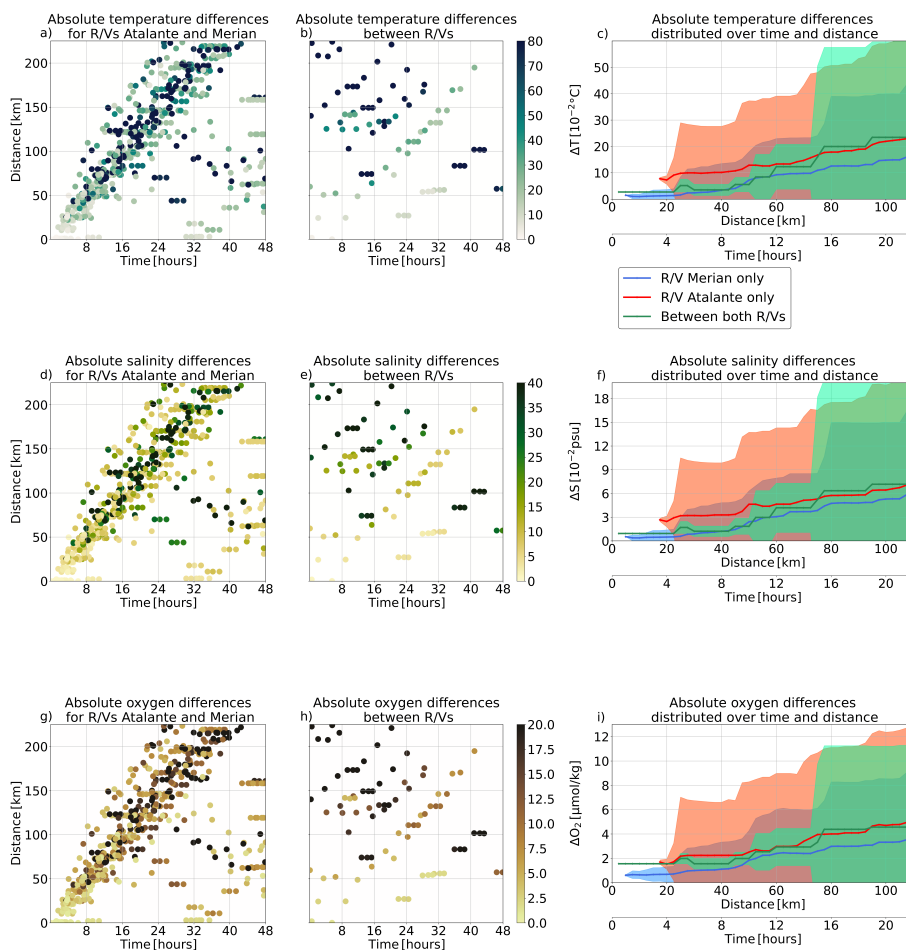


**Figure 5.** a) Absolute temperature differences between CTD pairs of profiles on isopycnal levels and averaged vertically distributed in time and distance. Each CTD pair is only composed of profiles from the R/Vs L'Atalante or Maria S. Merian. b) Same as a) but for CTD pairs composed of one profile from the R/V L'Atalante and one from the R/V Maria S. Merian. c) Temperature differences as a function of time and distance for CTD pairs from the R/Vs Maria S. Merian (blue), L'Atalante (red), and composed of one profile of each (green). d), e), and f) same as the above line but for absolute salinity differences, and g), h), and i) for absolute oxygen differences.

the measured parameters, these differences are found between those calculated for individual R/V, on average and standard variability, indicating that the uncertainty remains at a low order of magnitude. The same comparison performed between the R/Vs Maria S. Merian and Meteor shown on Figure 6 exhibits a small difference for temperature and salinity, but found within the standard deviation of the differences calculated for the individual ships. Nevertheless, for dissolved oxygen this difference is of  $3.5 \mu\text{mol/kg}$ , about the same order of magnitude of  $5 \mu\text{mol/kg}$  found for the uncertainty linked to the different calibration procedures.

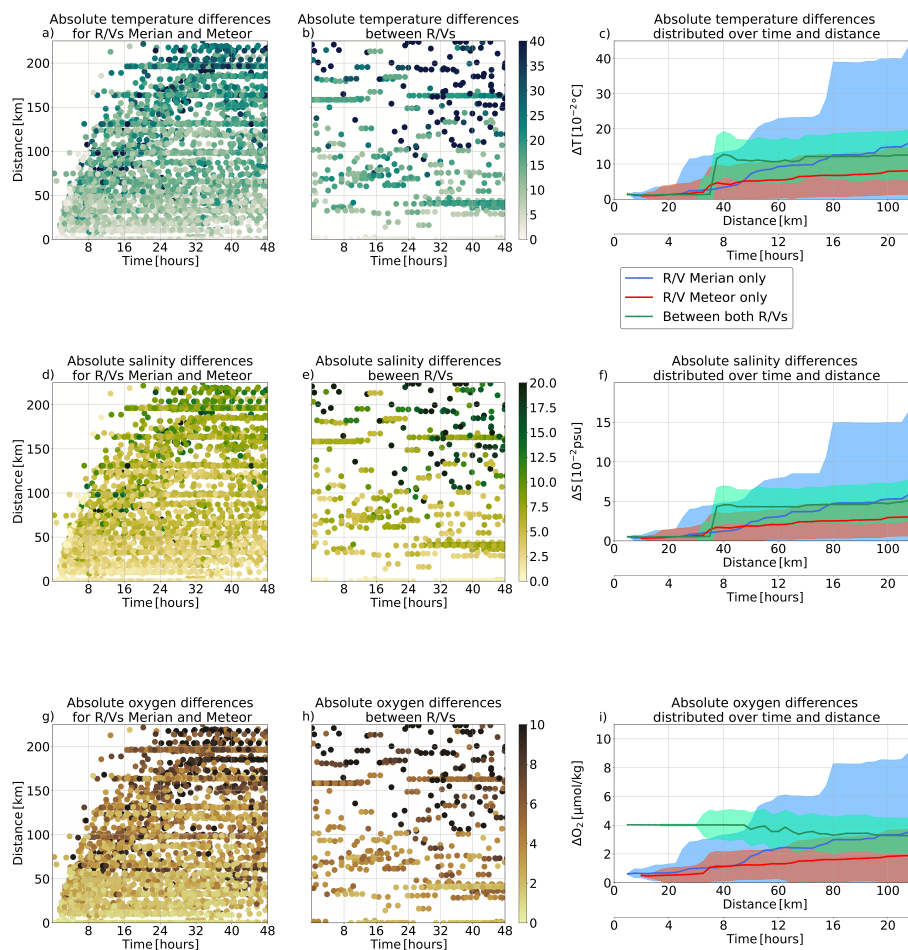


**Figure 6.** Same as Figure 5 but for the comparison between the R/Vs Maria S. Merian and Meteor.

### 3.3 Ship intake water analysis

#### 310 3.3.1 Thermosalinograph

The R/Vs L'Atalante and Meteor are equipped with Seabird SBE21 TSG, the R/V Maria S. Merian used two Seabird SBE45 TSG. These devices continuously measures temperature and salinity near the surface, between 6 and 7 meters of depth, depending on actual ship draught. The measurements are made at a frequency of 1 Hz and then averaged in 2-minute bins. Each day, a water sample is taken and analyzed aboard in order to adjust the salinity measurements. Figure 7 shows the positions of the TSG records during the EUREC<sup>4</sup>A-OA experiment.

As the measurements from this device are compared and corrected with actual water samples measured with level 1 sensors, the calibrated TSG records are at level 2 of our calibration hierarchy.

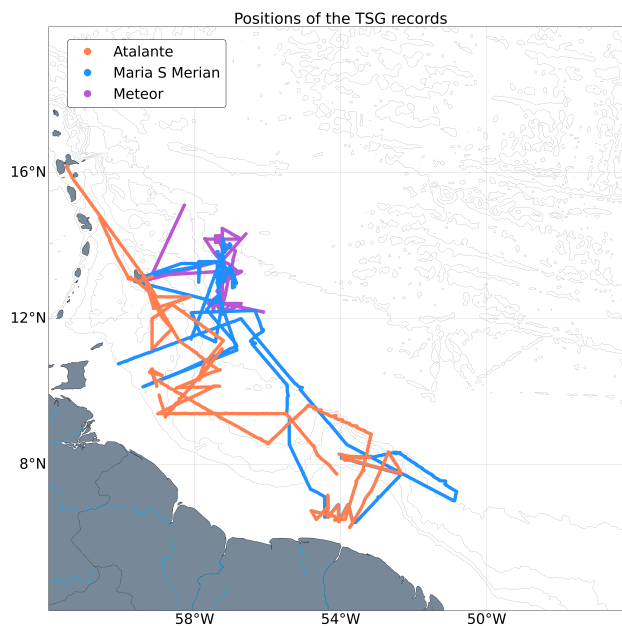


**Figure 7.** Map of the TSG records performed by the R/Vs L'Atalante, Maria S. Merian and Meteor.

The absolute differences for surface temperature and salinity, calculated from the TSG, are displayed on Figure 8. Compared to the CTD measurements (see Figures 5 and 6), the TSG resolution allows for finer spatio-temporal scales of observations. The R/Vs L'Atalante and Maria S. Merian captured on average the same absolute differences for both temperature and salinity, while the R/V L'Atalante presents larger standard deviation. Nevertheless, the difference calculated between the two ships remains on average around  $2 \cdot 10^{-2} \text{°C}$  and  $5 \cdot 10^{-2}$  psu above the ones calculated for each individual R/V. Similar offsets are found for the R/V Meteor (not shown). For temperature, the standard deviation of the difference calculated between the TSG of each R/V remains in the same range as the ones obtained for individual TSG, but for salinity it exceeds the individual TSG's ranges. These differences can be attributed to the calibration processes, to the differences between the two TSG types, and to the background oceanic variability. Overall, the uncertainty for the TSG assemble from all R/V is of  $2 \cdot 10^{-2} \text{°C}$  and  $5 \cdot 10^{-2}$  psu and is used for comparison with other devices measuring the surface with traceability of level 2 or below.

### 3.4 Underway CTD (uCTD)

An Ocean Science underway CTD system was used on the R/Vs L'Atalante and Maria S. Merian. The uCTD consists of a small winch system mounted on the bulwark of the ship and a CTD probe measuring temperature, conductivity, and pressure (Rudnick and Klinke, 2007). The probes sample at 16 Hz and data is recorded internally and read out onboard via a Bluetooth connection. This probe is designed to record data during descent, and the deployment procedure minimizes the influence of surface waves. The uCTD can be used in "free-cast" and "tow-yo" (or free fall) modes, depending on whether a winding line

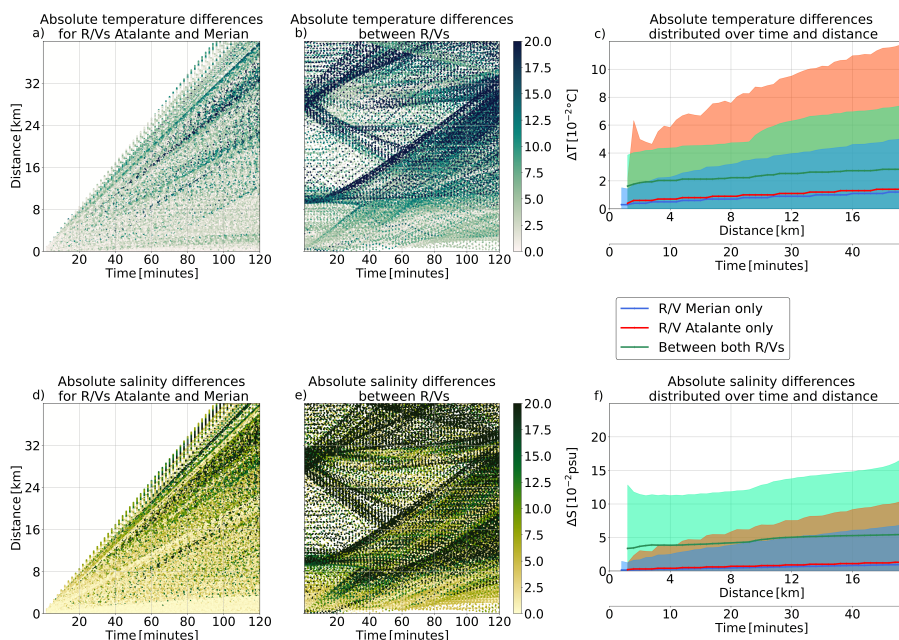


**Figure 8.** a) Absolute temperature differences between TSG pairs of measurements distributed in time and distance. Each TSG pair is only composed of measurements from the R/Vs L'Atalante or Maria S. Merian. b) Same as a) but for TSG pairs composed of one measurement from the R/V L'Atalante and one from R/V Maria S. Merian. c) Temperature differences as a function of time and distance for CTD pairs from the R/Vs Maria S. Merian (blue), L'Atalante (red), and composed of one profile of each (green). d), e), and f) same as the above line but for absolute salinity differences.

is either spooled or not onto the tail. In the first case, the probe descent is decoupled from the winch spool friction, keeping a rather steady descent rate of about 4 dbar/s. In the second mode, the probe fall rate is determined by the idle friction of the spool and the probe friction, and descent may vary between 3.5 dbar/s and about 0.6 dbar/s. For deployments of the uCTD from the R/V Maria S. Merian, both modes were used, with the "tow-yo" preferred for water depths shallower than 500 meters. 340 For deployments from the R/V L'Atalante, the uCTD was only deployed using the free fall mode, with no line spooled onto the tail. The difference in descent rate is an important factor to take into account in the calibration procedure, as the water is not pumped towards the sensors, contrary to what happens for sensors mounted on the CTD.

The R/V Maria S. Merian acquired a total of 380 profiles using three different uCTD probes, usually performed in series 345 with a drop every 30 minutes. The R/V L'Atalante carried out 179 uCTD profiles using two probes and usually alternating their deployment with CTD profiles. Figure 9a shows the positions of these profiles. Depending on the ship speed, the uCTDs sampled the water column between the surface and 300 to 500 meters of depth. Because no real-time information on the actual depth of the probe is available, the operator has to estimate the probe depth via cast time and estimated sinking velocity.



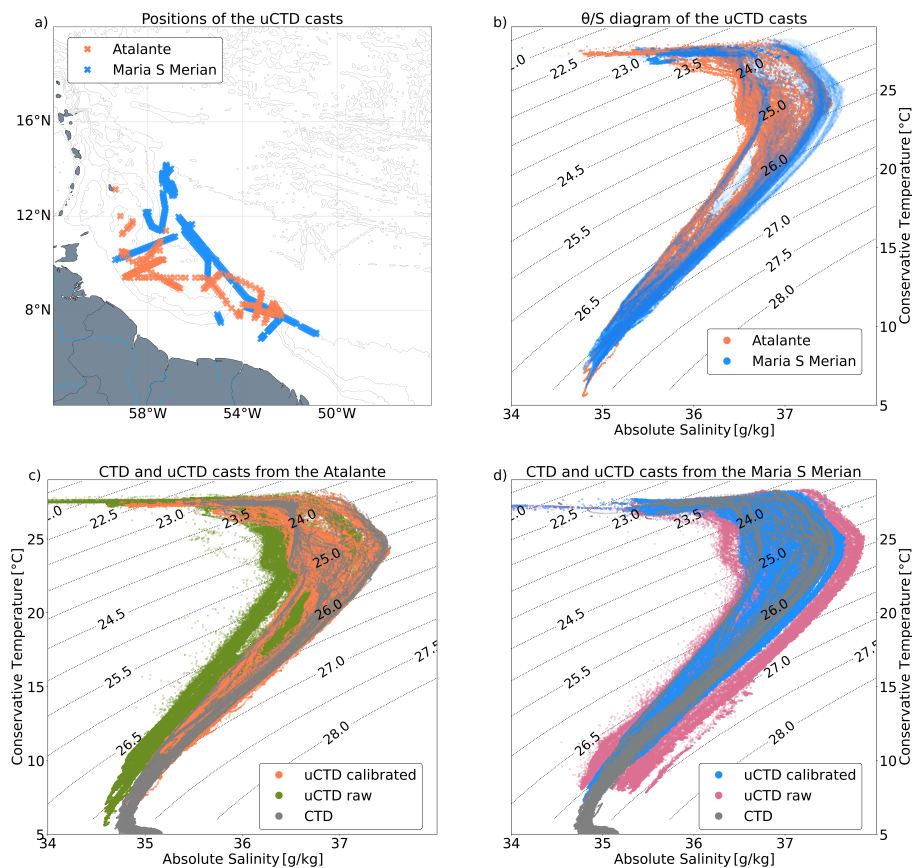


**Figure 9.** a) Map of the uCTD casts positions for the R/Vs L'Atalante and Maria S. Merian. b)  $\theta/S$  diagram of the uCTD profiles for each ship superimposed on the isopycnals. c) and d) Comparison of the raw and calibrated uCTD profiles superimposed on the CTD profiles for R/Vs L'Atalante and Maria S. Merian respectively.

350 There are four sources of salinity uncertainty associated with the uCTD measurements leading to errors of about  $4-5 \cdot 10^{-3} \text{ }^\circ\text{C}$ ,  
resulting in a computed salinity error of  $4-5 \cdot 10^{-3}$  psu (Ullman and Hebert, 2014). The first arises from a looping of the probe  
during which its direction reverses. The uCTD is made for recording data only during descent, so periods of inverse descent  
rate can be easily removed during the validation procedure. The second source of error comes from the variable fall rate of  
the probe. As the water is not pumped towards the sensors, there can be a lag in the measurements linked to the time it takes  
355 for the parcel of water to pass from one sensor to the other (Perkin et al., 1982; Lueck, 1990). Corrections are achieved via a  
minimization of this temporal lag, which depends on the fall rate. The third source of error is related to the strong deceleration  
of the probe when the spooled line reaches its end, leading to viscous heating of the thermistor. Larson and Pedersen (1996)  
provides a correction for this effect that is taken into account before computing salinity. The final source of error for salinity is  
detected as staggered changes when comparing the CTD profiles to those of the uCTD. Indeed, salinity values are lower for the  
360 uCTD than for CTD profiles when the temperature increases. This conductivity cell thermal mass error has been described in



Lueck (1990), and Lueck and Picklo (1990) proposed a correction based on the calculation of two parameters: the magnitude of the error  $\alpha$  and a time constant of the error  $\tau$ .

To perform the thermal mass correction, it is necessary to have close-by CTD/uCTD profiles. Specific profiles were also  
365 undertaken with the uCTD probe directly attached to the CTD rosette to gather the most synoptic measurements possible. Nevertheless, while the uCTD is designed to record the water column in a free fall mode, with the probe attached it is lowered at a constant but lower speed, and the presence of the rosette can disturb the flow near the sensor intake. As a consequence, even the co-located uCTD-CTD profiles can underestimate the error.

370 All corrections are performed using a Matlab toolbox based on Ullman and Hebert (2014). The procedure uses two separate calibrations: direct calibration of the uCTD probe attached to a CTD, giving nearly collocated uCTD and CTD profiles, and comparison with the TSG salinity. Figure 9b shows the calibrated profiles, and Figure 9c and d present their comparisons with CTD and raw uCTD profiles for each ship.

375 For the corrected uCTD, some calibration profiles were performed with the uCTD probe attached to the CTD rosette (level 3), while others were calibrated by comparing to nearby CTD stations (level 4), but since the correction is based on all available information we assign all profiles to level 4 of our calibration hierarchy. After correction of the uCTD data, we observe a clear improvement and agreement between the CTD and uCTD profiles. Figure 10 shows the vertically averaged differences between CTD and uCTD measurements for temperature and salinity for each individual R/V. Since the uCTD are calibrated with nearby  
380 CTD profiles it is particularly interesting to notice that the correction strongly reduces the differences in both temperature and salinity, for the mean and standard deviation, leading them closer to the differences as measured by only the CTD. For the R/V L'Atalante the comparison matches better than for the R/V Maria S. Merian, possibly linked to the deployment strategy, where uCTD and CTD measurements were alternately cast for the R/V L'Atalante, increasing the number of profiles to use as references for calibrations, while on the R/V Maria S. Merian full sections only used uCTD casts. The difference between the  
385 CTD only curve and the one combining CTD and uCTD provides an estimation of the uncertainty of  $9 \cdot 10^{-2} \text{ } ^\circ\text{C}$  and  $2 \cdot 10^{-2} \text{ psu}$  for the R/V Maria S. Merian, and  $6 \cdot 10^{-2} \text{ } ^\circ\text{C}$  and  $2 \cdot 10^{-2} \text{ psu}$  for the R/V L'Atalante.

### 3.5 Moving Vessel Profiler (MVP)

#### 3.5.1 Pressure, Temperature, Conductivity, and Salinity

390 A Moving Vessel Profiler (MVP) 30-350 from AML was operated on the R/Vs L'Atalante and Maria S. Merian. The MVP allows underway measurements from the surface down to a depth that depends strongly on the ship and water current speed, reaching a maximum of 350 meters. The MVP 30-350 consists of an electric winch system, a PC control unit and the towed vehicle ("fish") that can be equipped with different sensors. A conductive probe provides real-time data access. The "fish" is

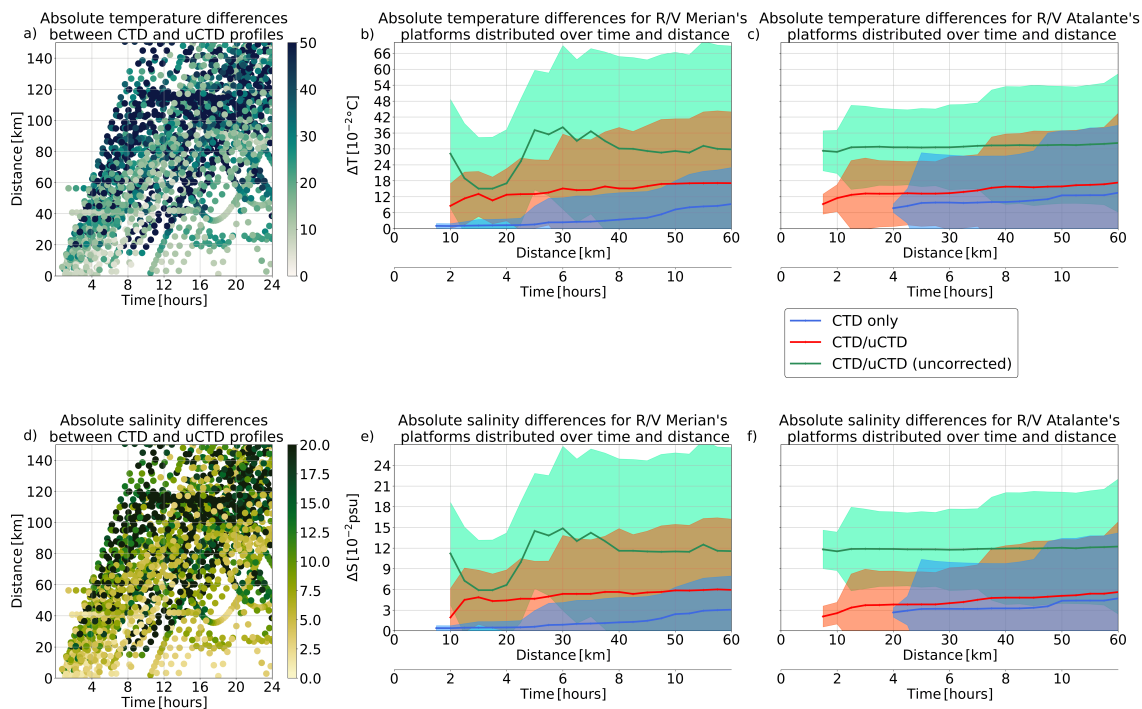


**Figure 10.** a) Absolute temperature differences between CTD/uCTD pairs of profiles on isopycnal levels and averaged vertically distributed in time and distance. Each pair is composed of profiles from the same R/V, one CTD and one uCTD. b) Temperature differences as a function of time and distance for pairs of profiles from the R/Vs Maria S. Merian. In blue for pairs of CTD only profiles, in red for pairs composed of one CTD and one uCTD profiles, and in green for pairs composed of one CTD and one uncalibrated uCTD profiles. c) Same as b) but for the R/V L'Atalante. d), e), and f) same as the above line but for absolute salinity differences.

forced to rapidly (up to 2 m/sec) descend and ascend with the help of a tail-unit. The fish design enables descent, ascent, and  
 395 drag phase (time before the next descent) data recordings to be used.

The MVP deployed from the R/V Maria S. Merian performed 1891 profiles with ship speed from 2 to 10 kn (mean 6.9 kn). The MVP deployed from the R/V L'Atalante completed 1960 profiles (Figure 11a). The device was operated in different areas and guided by dynamical features (mesoscale eddies, filaments, frontal regions). In regions with a shallow topography, the maximal diving depth was either controlled by an operator (real-time data) or by feeding the bottom topography (e.g., from the  
 400 ships' echo sounder) into the MVP control unit (as done on Maria S. Merian in shallow topography and requesting the fish to ascend when reaching a depth of 10 m above the seafloor). On the R/V Maria S. Merian the MVP was also equipped with a fluorescence sensor.

The CTD sensors on the MVP are affected by similar sources of error as the uCTD and the ship CTD: the speed of the probe  
 405 through the water, CT time-lag, and thermal mass, and a similar calibration strategy is therefore used for the MVP sensors. The

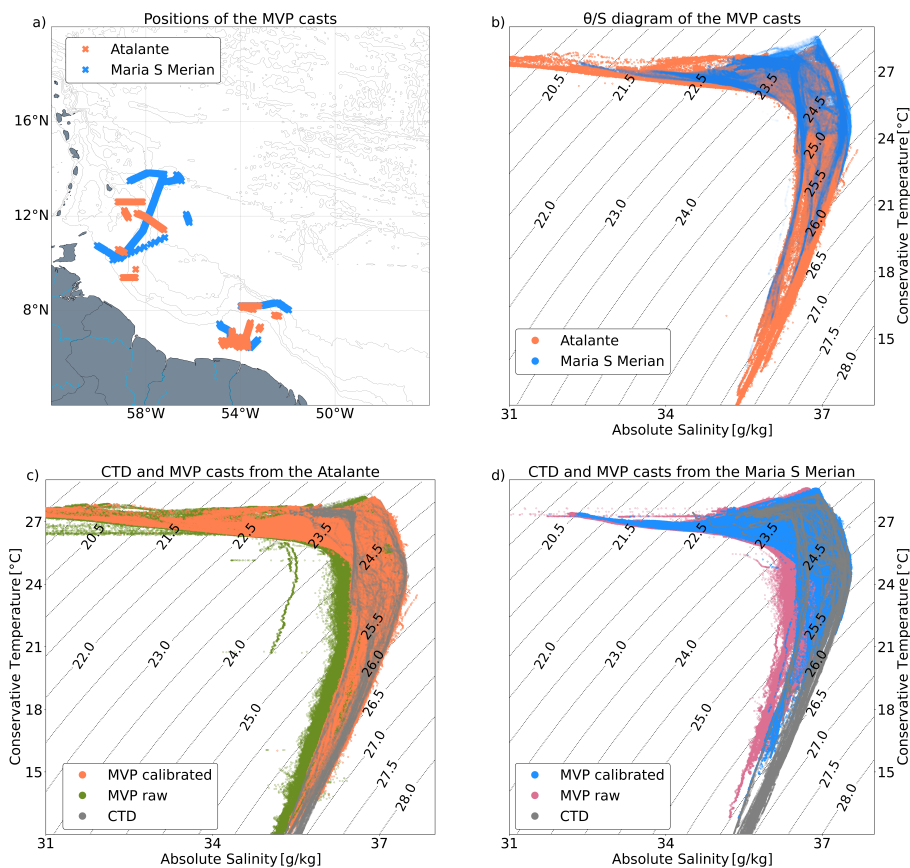


**Figure 11.** a) Map of the MVP casts positions for the R/Vs L'Atalante and Maria S. Merian. b)  $\theta/S$  diagram of the MVP profiles for each ship superimposed on the isopycnals. c) and d) Comparison of the raw and calibrated MVP profiles superimposed on the CTD profiles for the R/Vs L'Atalante and Maria S. Merian respectively.

MVP also appears to be sensitive to surface waves. We therefore removed them by applying a low-pass filter with a cut-off frequency calculated from the surface waves. As explained in the uCTD section, the temporal lag and thermal mass errors are linked respectively to the vertical speed and the time match between conductivity and temperature pairs. In order to perform this calibration, we calculated downward and upward correction coefficients based on the method from Mensah et al. (2018).  
 410 The calibration resulted in a good match between nearby ship CTD and CTD sensors on the MVP (Figure 11c, d).

Because the calibration takes into account only nearby CTD profiles, temperature, salinity, and pressure measurements are ranked level 4 of traceability. We observe (Figure 12) that the averaged differences between nearby CTD profiles, and standard deviations reduce after calibration. As for the uCTD comparisons with the CTD, a difference between CTD only and  
 415 MVP/CTD ones subsists. Again, this is attributed to the different devices' deployment, the sampling strategy and the oceanic variability of the regions measured. The estimated uncertainty for the corrected MVP is of  $6 \cdot 10^{-2} \text{°C}$ , and  $3 \cdot 10^{-2} \text{psu}$  for the

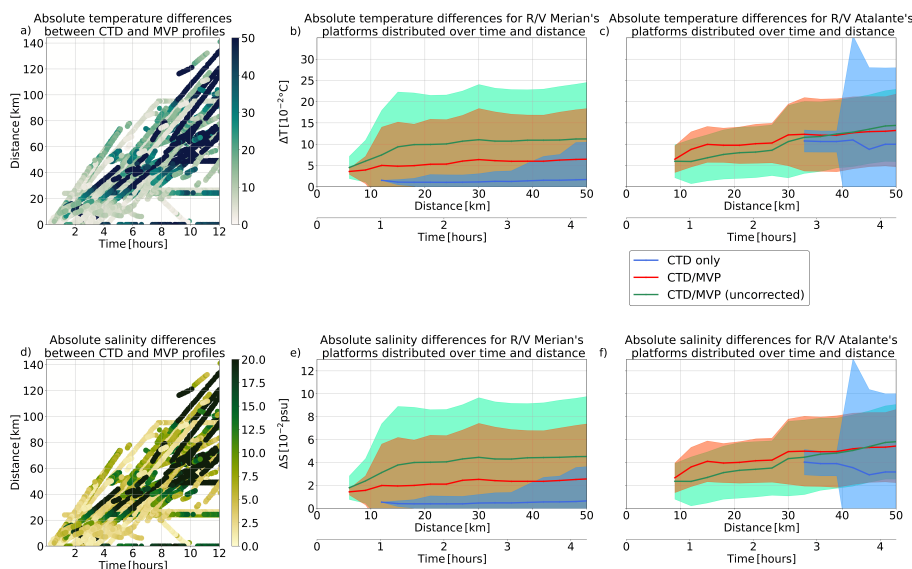


**Figure 12.** a) Absolute temperature differences between CTD/MVP pairs of profiles on isopycnal levels and averaged vertically distributed in time and distance. Each pair is composed of profiles from the same R/V, one CTD and one MVP. b) Temperature differences as a function of time and distance for pairs of profiles from the R/V Maria S. Merian. In blue for pairs of CTD only profiles, in red for pairs composed of one CTD and one MVP profiles, and in green for pairs composed of one CTD and one uncalibrated MVP profiles. c) Same as b) but for the R/V L'Atalante. d), e), and f) same as the above line but for absolute salinity differences.

R/V L'Atalante, and  $4 \cdot 10^{-2} \text{ } ^\circ\text{C}$ , and  $2 \cdot 10^{-2}$  psu for the R/V Maria S. Merian.

### 3.6 Ship mounted ADCP (S-ADCP)

420 Upper ocean currents were measured quasi-continuously with Teledyne RD Instruments Ocean Surveyor Acoustic Doppler Current profiler (S-ADCP). On all three ships a 38 kHz ADCP was operated, measuring velocities from around 50 to some-  
 times even below 1000 meters depth depending on availability of scatters. The R/Vs Meteor and Maria S. Merian were also  
 equipped with a 75 kHz ADCP, providing measurements between 40 and 800 meters of depth with a finer resolution compared  
 to the 38 kHz S-ADCP. The R/V L'Atalante, on the other hand, was equipped with a 150 kHz ADCP, supposedly ranging  
 425 from around 20 meters to 400 meters depth. However, this ADCP rarely reached water depths below 200 meters during the  
 experiment. The ADCP accuracy is  $\pm 5\%$  of measured velocity or  $\pm 0.5$  cm/s, whichever is greater.

During the experiment, on a daily basis, data from the R/V L'Atalante were then processed with the CASCADE software  
 developed by IFREMER (Le Bot et al., 2011; Speich et al., 2021). The data from the R/Vs Maria S. Merian and Meteor was  
 430 processed using a set of Matlab routines applied to the raw data, meaning the data was sampled in an as-fast-as-possible mode



(approximately 1HZ).

To enable a direct comparison of the measurements from all ships, the ADCP data was reprocessed using the UHDAS routines Firing et al. (2012). This comparison did not show any notable difference among the data sets. The final data set consists  
435 of zonal and meridional velocities averaged in two-minutes segments. As the device is directly mounted on the hull of the ships, the measurements follow the same tracks as the TSG (Figure 7).

By default, we place the calibrated S-ADCP measurements on the second level of our hierarchy, since only an intercomparison between devices can be done and no comparison with a reference is possible. The L-ADCP measurements are placed one  
440 level below (level 3), since S-ADCP measurements are used as reference.

## 4 Autonomous devices

### 4.1 Underwater Gliders

#### 4.1.1 Pressure, Temperature, Conductivity, and Salinity

445 During the experiment, 7 underwater gliders were deployed (Figure 13). From the R/V L'Atalante a SeaExplorer Glider, named Kraken, was deployed and carried out 831 profiles to a maximum depth of 700 meters in 15 days of operation. The glider was deployed to cross along different quadrants of a mesoscale eddy previously located in satellite altimetry maps. Its CTD, a Glider Payload CTD, has an accuracy of  $4 \cdot 10^{-3}^{\circ}\text{C}$  for temperature and of  $1 \cdot 10^{-3} \text{ mS/cm}$  for conductivity.

From the R/V Maria S. Merian, 3 autonomous gliders (IFM03, IFM09, IFM12) have been deployed. IFM09 conducted  
450 327 profiles to a maximum depth of 900 meters in 20 days following a quasi-stationary mode in the trade-wind alley area. IFM03 and IFM12 were deployed in the northeastern region of a mesoscale eddy, performing respectively 125 and 443 profiles down to a maximum depth of 900 meters in 6 and 24 days, respectively. Due to a leak, IFM03 was retrieved by the R/V Meteor.

Three gliders from the University of East Anglia (UEA) collected profiles with an "hourglass" sampling pattern. The gliders  
455 (SG579, SG620, SG641) collected 442, 262 and 308 profiles for 10, 13 and 24 days down to maximum depths of 950, 750 and 750 meters, respectively.

While the sensor suites on the gliders varied, all were equipped with Seabird CTDs. (Stevens et al., 2021). The underwater gliders are subject to the same sources of errors as all the previously described undulating probes. Nevertheless, the rising and  
460 descending profiles are performed at a much lower speed compared to the free-fall of the uCTD. For some devices the water was pumped through the CTD and this controlled flow strongly diminished the viscous heating and temporal lag effects. For others this was not the case and the flow speed was estimated by determining the speed of movement through the water based

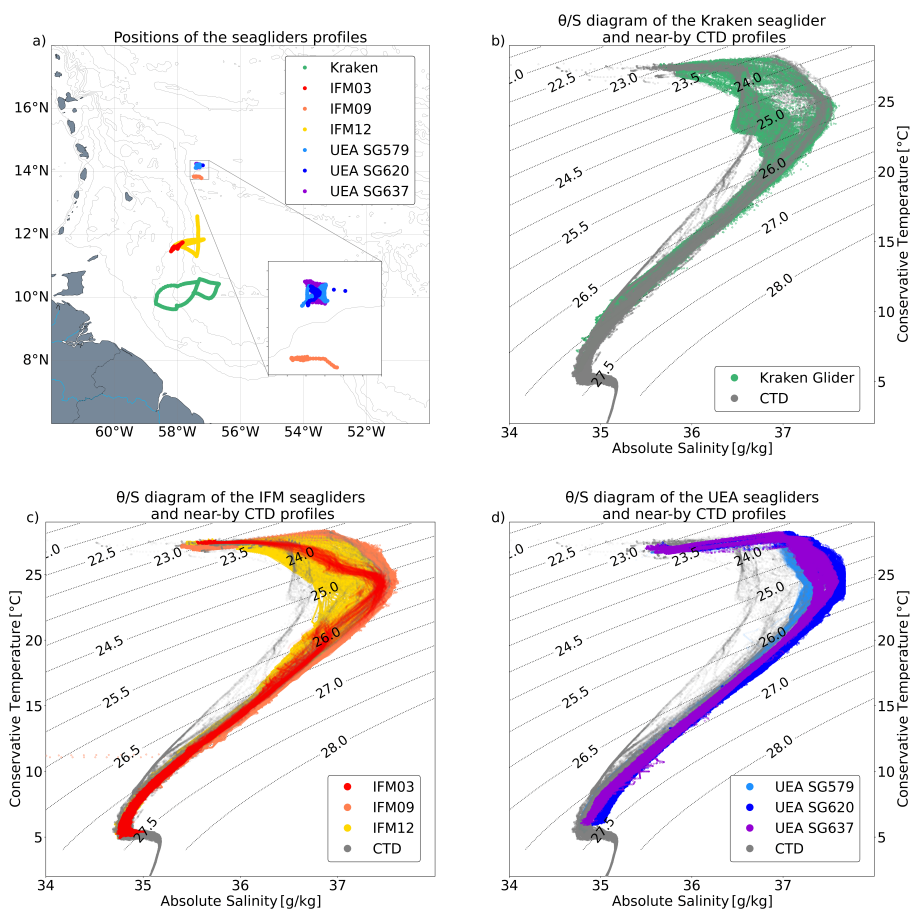


**Figure 13.** a) Map of the 7 underwater gliders positions. b)  $\theta/S$  diagram of the Kraken glider measurements, deployed from the R/V L'Atalante, compared to near-by CTD casts. c) Same as b) for the IFM gliders deployed from the R/V Maria S. Merian. d) Same as b) for the University of East Anglia gliders deployed from the R/V Meteor.

on an optimized glider travel model.

465 In principle, similar correction procedures were used for the MVP and underwater gliders. These were necessary to avoid  
 any misalignment between the downward and upward profiles, taking into account the flight model, and to have coherent cali-  
 470 brations across the platforms.

No direct or lab calibration was done with the glider CTD sensors; instead, data calibration was performed through com-  
 470 parison with nearby (time, space) CTD stations. To ease comparison we group all three UEA Seaglider, the IFM gliders, and  
 the Kraken (Figure 14 above and middle line panels). The number of close-by pairs of CTD and glider profiles is quite low for  
 the Kraken. Nevertheless, the mean differences for pairs of profiles found closer than 30 km are less than 30 km are below 2

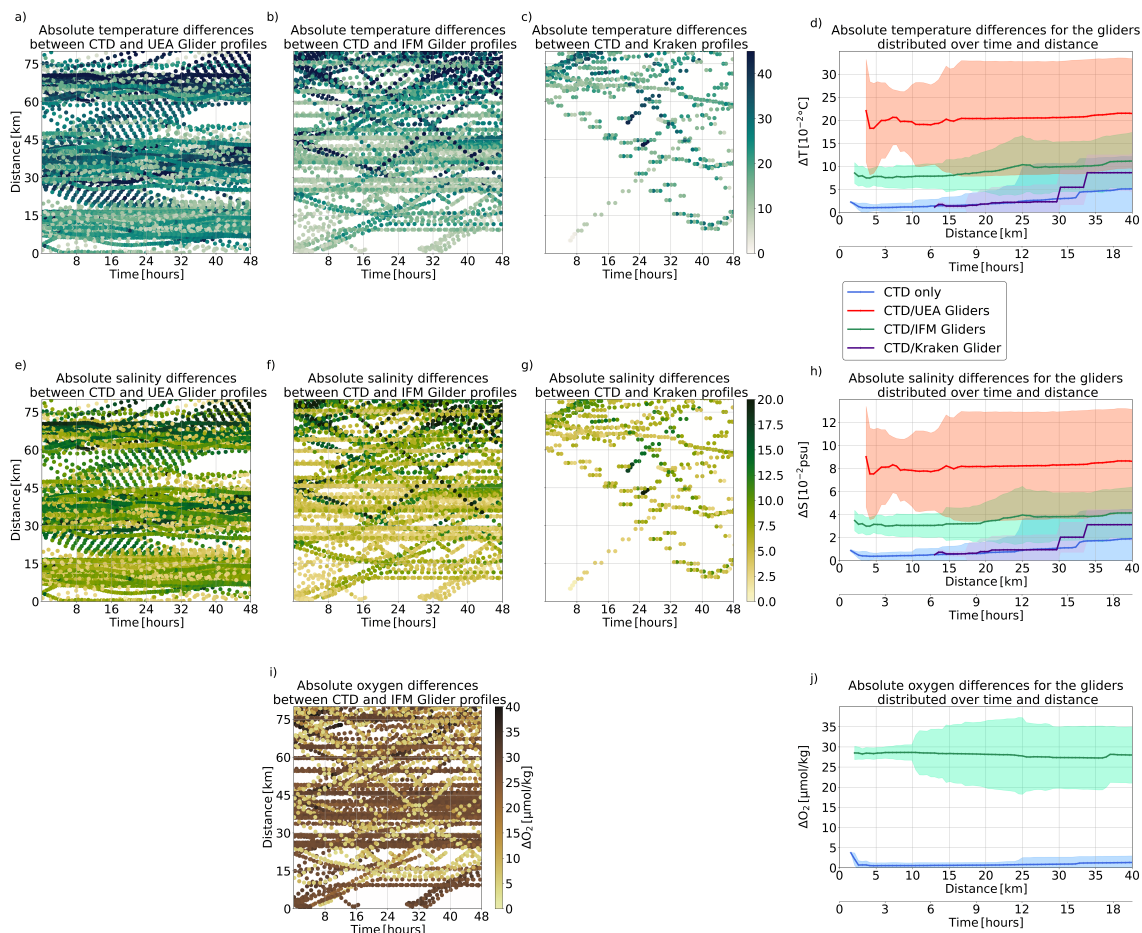


**Figure 14.** a), b), and c) Absolute temperature differences between CTD/Glider pairs of profiles on isopycnal levels and averaged vertically distributed in time and distance. Each pair is composed of one CTD and one Glider profiles. Respectively a), b), and c), correspond to the UEA, IFM, and Kraken Gliders. d) Temperature differences as a function of time and distance for pairs of profiles. In blue for pairs of CTD only profiles, in red for pairs composed of one CTD and one UEA profiles, in green for pairs composed of one CTD and one IFM profiles, and in purple for pairs composed of one CTD and one Kraken profiles. The middle line of panels e) to h) is the same as above, but for absolute salinity differences. The bottom line of panels correspond to absolute oxygen differences, but only IFM Gliders measured dissolved oxygen.

475  $10^{-2}^{\circ}\text{C}$ , and  $1 \cdot 10^{-2}$  psu. The IFM gliders tend to constant positive bias in temperature and salinity compared to the near-by CTD stations, with a low standard deviation despite having a higher number of pairs of profiles. Within the first 15 km the uncertainty is on the order of  $8 \cdot 10^{-2}^{\circ}\text{C}$ , and  $3 \cdot 10^{-2}$  psu. The UEA Seaglider shows stronger differences in temperature and salinity associated with a strong standard deviation. These values can be attributed to the calibration and differences between devices but also to the sampling strategy; the pairs UEA Seaglider/CTD are mostly composed of the stations performed by the R/V Meteor, close to each other (see Figure 3a) thus possibly capturing finer scales variability. Their uncertainty is here estimated at





0.2°C and  $8 \cdot 10^{-2}$  psu). As for the MVP measurements, the underwater gliders are placed at level 4 on the calibration hierarchy.  
480

#### 4.1.2 Dissolved Oxygen

The three IFM gliders were equipped with AADI Aanderaa optodes of type 3830 (IFM03, IFM09) and type 4831 (IFM12). The manufacture-provided resolution and accuracy for oxygen concentration are 1 mmol and 8M or 5% (whichever is greater, concentration) and  $< 5\%$  (air saturation). For the three IFM gliders, lab calibrations of the oxygen sensors were done on  
485 board the Maria S. Merian by preparing zero (chemically forced) and 100% saturation (air bubbles injected) water of two temperatures, following the Aanderaa optode manual. The resultant readings were used to constrain the phase / temperature relation of the foil.

Figure 14g) provides information about oxygen concentration with, on average, negative (not shown) differences of  $28 \mu\text{mol/kg}$ . However, this relatively strong uncertainty value has to be put in perspective with the associated standard deviation of about  
490  $\pm 2 \mu\text{mol/kg}$  for CTD/Glider pairs found within 10 km, suggesting a rather constant bias in the sensors.

#### 4.1.3 Other sensors

CDOM optical sensors were mounted on the IFM12, SG579, and Kraken gliders to estimate dissolved organic matter. A SUNA nutrient analyzer was used on IFM12. IFM03 and SG620 were equipped with a Rockland Scientific MicroRider turbulence  
495 sensor to estimate small-scale mixing. The SG637 glider was equipped with a Nortek Signature1000 1 MHz ADCP to measure the vertical shear of horizontal currents. None of these sensors is considered here.

### 4.2 Saildrones

#### 4.2.1 Pressure, Temperature, Conductivity, and Salinity

With the objective of measuring the surface from both the atmospheric and oceanic perspectives, five Saildrones were deployed,  
500 three funded by NASA and two by NOAA. Below the water line, a pumped CTD (SBE-37-SMP-ODO Microcat) measured temperature, conductivity, and dissolved oxygen at 0.5 meter depth, and they were also equipped with a chlorophyll-a sensor (Wetlabs ECO-FL-S G4 and Turner Cyclops). A Teledyne Workhorse 300kHz ADCP was mounted on the NASA Saildrones to measure the current velocity from 6 to 100 meters depth. Their nominal accuracies are  $\pm 2 \cdot 10^{-3} \text{°C}$  for temperature,  $\pm 3 \cdot 10^{-3}$  mS/cm for conductivity,  $\pm 3 \mu\text{mol/kg}$  or  $\pm 2\%$  for dissolved oxygen, and  $2 \cdot 10^{-2} \mu\text{g/l}$  for chlorophyll-a. These values  
505 have the same order of magnitude as those for the sensors mounted on the CTD probes. The ADCP accuracy is  $\pm 5\%$  of measured velocity or  $\pm 0.5$  cm/s, similar to that of the S-ADCPs. The Saildrones are autonomous and operated remotely, and their measurements are valuable as they provide 1-minute averaged records of temperature and salinity near the sea surface, and 5-minute averaged records of velocity with high vertical resolution in the upper layer of the water column. Nevertheless, calibrations were only made in laboratory before and after the mission, as direct comparisons with water samples are impossible;

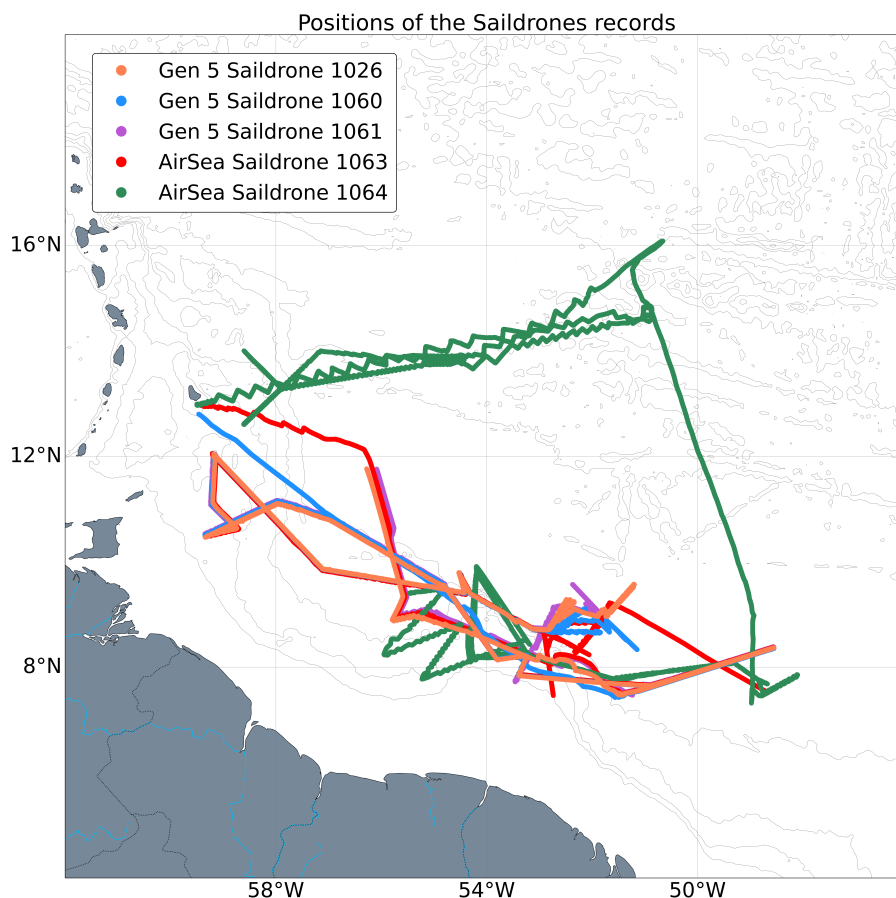


**Figure 15.** Map of the five Saildrones positions. Three NASA Saildrones (1026, 1060 and 1061) and one NOAA Saildrone (1063) have followed the R/Vs Maria S. Merian and L'Atalante tracks to sample surface mesoscale eddies, while one NOAA Saildrone (1064) has first sampled the trade wind alley.

510 as such, we place the Saildrones on level 4 of our calibration hierarchy.

As for the previous devices, Figure 16 shows the comparison between the temperature and salinity measurements made by the Saildrones and the near-surface values from the R/Vs L'Atalante and Maria S. Merian measurements. The Saildrones followed their own routes away from the ships, nevertheless the high frequency of acquisition provides enough nearby measurements for comparison. For calibration purposes, 4 of the 5 Saildrones spent times twice near the R/V L'Atalante. For temperature, measurements found below 1 km apart show difference of about  $3 \cdot 10^{-2} \text{ } ^\circ\text{C}$  before reducing and following the R/Vs' TSG tendency with a difference of  $1 \cdot 10^{-2} \text{ } ^\circ\text{C}$ . For salinity, the same evolution is found, with a difference climbing to  $5 \cdot 10^{-2}$  psu for measurements found within 1 km, before reducing and keeping an offset of less than  $1 \cdot 10^{-2}$  psu with the R/Vs'

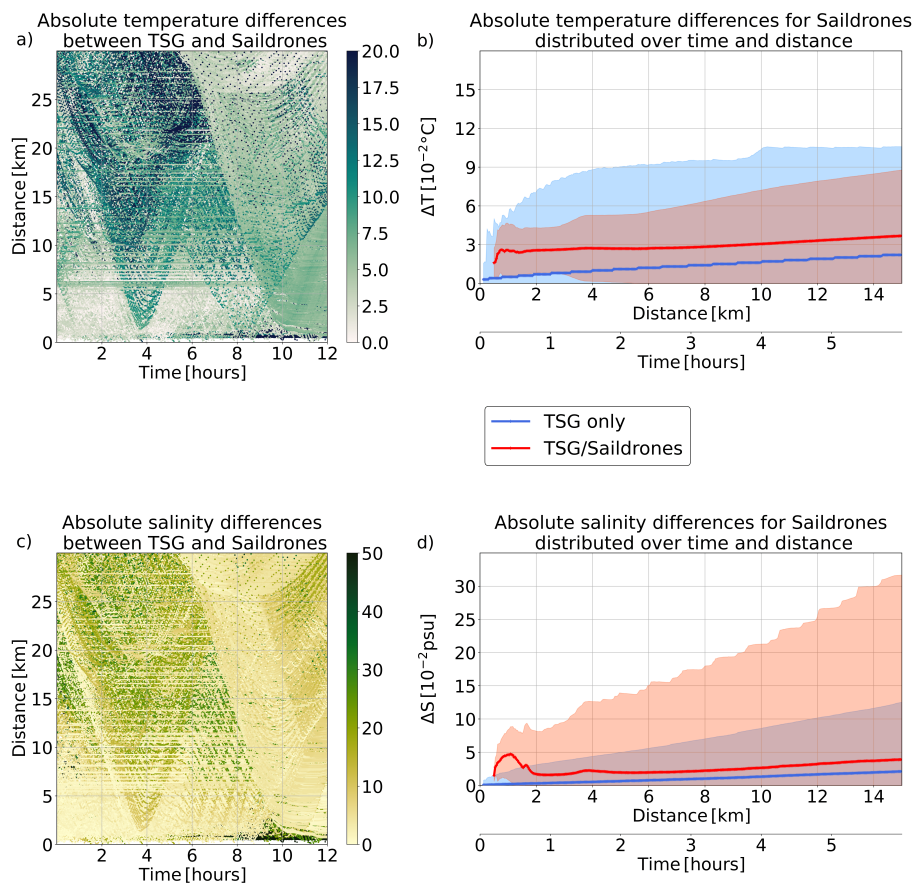


**Figure 16.** a) Absolute temperature differences between TSG/Saildrone pairs of measurements distributed in time and distance. Each pair is composed of one R/V's TSG measurement and a Saildrone's one. b) Temperature differences as a function of time and distance for a pair of surface measurements. In blue for pairs of R/Vs' TSG only profiles, in red for pairs composed of one R/V's TSG and one Saildrone's. c) and d), same as the above line, but for absolute salinity differences.

TSG.

520

### 4.3 Argo floats

#### 4.3.1 Pressure, Temperature, Conductivity, and Salinity

During the experiment, 5 Argo floats were deployed from the R/V L'Atalante. As seen in Figure 17, only a very limited number of profiling floats drifted in the region in late 2019 and early 2020. Two of the deployed Argo floats were configured to follow a large surface-intensified mesoscale anticyclone, one was deployed in a region between two mesoscale eddies, and the two within a subsurface anticyclone. The positions of the deployments were determined from analyses of satellite altimetry maps

525

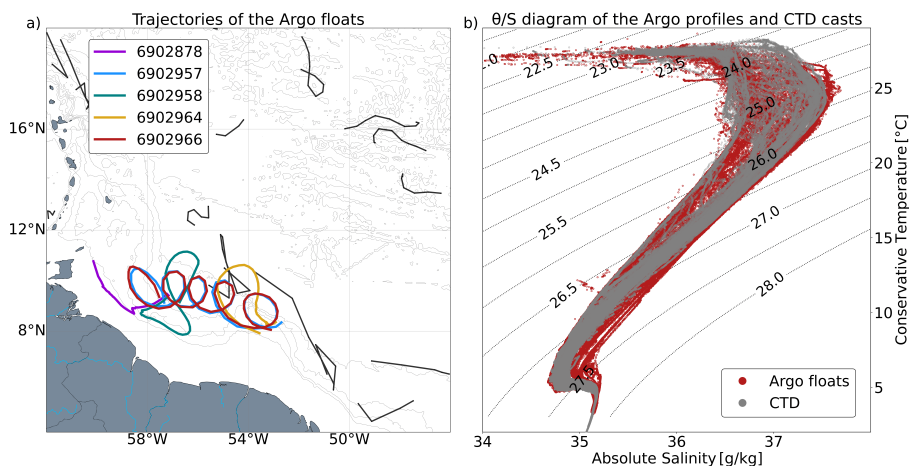


**Figure 17.** a) Map of the Argo floats found in the region of interest between December 2019 and May 2020; specific colors are attributed to the five floats deployed from the R/V L'Atalante. b)  $\theta/S$  diagram of the Argo floats, compared to near-by CTD casts, no clear bias is observed here.

and the detection of eddies with the TOEddies algorithm (Laxenaire et al., 2018), as well as with the analyses of S-ADCP data from the different ships. The floats were initially set to perform daily vertical profiles between 0 and 1000 meters depth, and when not profiling they were positioned to a parking depth at 200 dbar. After a period varying between 10 and 90 days, they were programmed to the core Argo setting (a parking depth of 1000 dbar and vertical profiles every 10 days between 2000 dbar and the surface). Their trajectories and vertical profiles were collected and validated by the Coriolis Argo Global Data Assembly Center (GDAC) Argo (2000). These 5 floats are PROVOR manufactured by NKE. They were equipped with Seabird CTD sensors SBE41, and their positions were transmitted via the Iridium system. They measured pressure, temperature, and salinity with respective accuracy of  $\pm 2.4$  dbar,  $\pm 2 \cdot 10^{-4}$  °C, and  $\pm 3 \cdot 10^{-3}$  psu. Each of the sensors may drift over the years, but any drift remained small over the period of the experiment.

As Figure 18 underlines, direct comparisons between Argo floats and nearby CTD stations are limited because of the low number of measurements. Moreover, since the float trajectories differ strongly from that of the ship, the background oceanic variability estimated from the CTD might differ. Nevertheless, for nearby pairs of Argo and CTD profiles, the difference remains small. For ARGO floats and CTD stations found within 50 km, the uncertainties for temperature and salinity are of  $9 \cdot 10^{-2}$  °C and  $2 \cdot 10^{-2}$  psu. These uncertainties are of the same order of magnitude as those quantified for the other level 4 devices sampling the water column (uCTD and MVP).

### 4.3.2 Dissolved Oxygen

Additionally, an OPTODE sensor (for dissolved oxygen) from AANDERAA with an accuracy of  $4 \mu\text{mol/kg}$  was mounted on the Argo floats deployed from R/V L'Atalante. In the same spatial and temporal range as the CTD stations, the dissolved



oxygen sensors exhibit an uncertainty of  $11 \mu\text{mol/kg}$  for a 50 km range (see Figure 18f).

#### 4.4 Surface Drifters

Four kinds of surface drifters were deployed from the R/V L'Atalante during the experiment. Two SURPACT drifters were  
550 launched for short periods of time, less than two days, and we will not describe them in detail here. Five SVP-BRST drifters  
from Eumetsat grant TRUSTED to MétéoFrance/CLS, measured temperature at 0.15 meters depth, with an accuracy of  
 $\pm 5^{-3}^{\circ}\text{C}$ . Two SVP-BSC drifters from MétéoFrance/LOCEAN with CNES SMOS support measured temperature and salinity  
at 0.2 meters depth, with respective accuracy of  $\pm 0.1^{\circ}\text{C}$  and  $\pm 5^{-2}$  psu, configured to send data every 6 minutes with a sampling  
rate of 20 seconds. Finally, ten SVP-BSW drifters from NOAA were deployed to measure temperature and salinity, at 0.5, 5  
555 and, 10 meters of depth with the same accuracy as SVP-BSC drifters, transmitting data every 30 minutes. Figure 19 shows the  
positions of these drifters, exhibiting clear advection toward the Northwest, with some of them looping.

From the R/V L'Atalante, two SVP-BSC and Surpact were deployed for short periods of time to compare their measure-  
ments with the similar devices and nearby instruments (Reverdin et al., 2021). Figure 20, similar to that for Saildrones, shows  
560 the comparison between surface TSG measurements and nearby drifter records. As for the Saildrones, these comparisons are  
delicate because the drifters measured temperature and salinity at different vertical levels near the surface, capturing a sensibly  
different background variability. The observed difference for the SVP-BSW drifters remains small for near-by pairs of mea-  
surements (less than 5 km apart), with an uncertainty of  $3 \cdot 10^{-2}^{\circ}\text{C}$  for temperature and  $3 \cdot 10^{-2}$  psu for salinity. The SVP-BSC  
drifters' measurements exhibit a large difference in both temperature and salinity,  $6 \cdot 10^{-2}^{\circ}\text{C}$  and  $3 \cdot 10^{-1}$  psu, particularly linked  
565 to one drifter. This is related to a large thermal effect upon deployment, supposedly becoming near negligible after a few hours.  
The manufacturer states that we should not consider the first few hours of data. Finally, temperature measurements from the  
SVP-BRST drifters follow the uncertainty from the TSG only, with an offset of about  $3 \cdot 10^{-2}^{\circ}\text{C}$ .

#### 5 Data Concatenation

All the measured and cross-validated parameters can be associated with a level of uncertainty while using a concatenated  
570 dataset. For example, for a vertical section of salinity using CTD, uCTD, and MVP measurements, the associated uncertainties  
are  $3 \cdot 10^{-2}$  psu for the uCTD and  $2 \cdot 10^{-2}$  psu for the MVP. Thus, the dataset provides an array with the different uncertainties  
for each type of profile.

The concatenated data are very useful for enhancing the space-time resolution of many of the sampled areas and for better  
575 assessing dynamical properties of the regional ocean circulation. With these data it is, for example, possible to assess relevant  
properties of surface and subsurface mesoscale eddies, freshwater filaments, cold water pools and freshwater-induced barrier  
layers. Figure 21 shows the impact of the calibration on a specific section performed by the R/V L'Atalante using CTD, uCTD,



and MVP measurements. The first column, displaying only the CTD profiles, has a coarse horizontal resolution but is associated with low uncertainty linked to the validation and calibration processes. The second row presents the complete section, with the uncalibrated MVP and uCTD profiles. There we observe an increase in the horizontal resolution but nevertheless find some inconsistencies, as seen in panels b and c with strong variations between two successive profiles of salinity and potential density. Finally, after calibration, as seen in the last column, the uCTD and MVP profiles are corrected and cross-validated with the CTD measurements. The inconsistencies are removed while still keeping high horizontal resolution and low uncertainty, enabling the calculation of realistic gradients of the different fields and the analyses of derived parameters, such as the Ertel Potential Vorticity (see Figure 21, panel e).

## 6 Data availability

The underlying primary CTD and TSG datasets, used in this study for comparison with other devices, are available for each R/V on the AERIS website (<https://observations.ipsl.fr/aeris/eurec4a/#/>). Additionally, for the R/V L'Atalante, the CTD measurements can be retrieved on the Seanoë website (<https://doi.org/10.17882/79096>) (Speich et al., 2021). Calibrated TSG measurements for the R/Vs Maria S. Merian and Meteor are available on the Pangea website under the cruise names of MSM89 (<https://doi.pangaea.de/10.1594/PANGAEA.951515>) and M161 (<https://doi.pangaea.de/10.1594/PANGAEA.951515>) respectively (Karstensen et al., 2020; Mohr et al., 2020).

After the secondary data quality control process was applied, the various data sets were interpolated to the same vertical pressure grid with a 0.5 dbar resolution. This was done for temperature, salinity, and dissolved oxygen data and, when available, horizontal ocean currents. For each device, a NetCDF file is available for download on the Seanoë website, organized by type of device and ship, with its own DOI. The naming of the variables and parameters follows the convention of the NetCDF Climate and Forecast (CF) Metadata Conventions Eaton et al. (2003). The secondary quality control uCTD and MVP profiles can be found on the Seanoë website (<https://doi.org/10.17882/91352> and <https://doi.org/10.17882/91485> respectively). Additionally, the concatenated sections described in the previous section, composed of CTD, secondary quality control uCTD and MVP profiles, and S-ADCP measurements from the R/Vs L'Atalante and Maria S. Merian can be accessed on the Seanoë website (<https://doi.org/10.17882/92071>).

Measurements from the autonomous devices, Saildrones, underwater gliders and drifters can also be retrieved from the AERIS website (<https://observations.ipsl.fr/aeris/eurec4a/#/>). Furthermore, the UEA gliders measurements are available on the British Oceanographic Data Center website (doi:10.5285/c596cdd7-c709-461a-e053-6c86abc0c127). Data from the Argo floats are available on the Coriolis website (<https://dataselection.coriolis.eu.org/>). Table 1 summarizes the different links and DOIs to access these various datasets.

610



<b>Vertical Profiles</b>		
<b>Platforms</b>	<b>Parameters</b>	<b>DOI/Access Data</b>
R/V L'Atalante CTD	Temperature/Salinity/Oxygen	<a href="https://doi.org/10.17882/79096">https://doi.org/10.17882/79096</a>
R/Vs Maria S. Merian and Meteor CTD	Temperature/Salinity/Oxygen	<a href="https://observations.ipsl.fr/aeris/eurec4a/#/">https://observations.ipsl.fr/aeris/eurec4a/#/</a>
R/Vs L'Atalante and Maria S. Merian uCTD	Temperature/Salinity	<a href="https://doi.org/10.17882/91352">https://doi.org/10.17882/91352</a>
R/Vs L'Atalante and Maria S. Merian MVP	Temperature/Salinity	<a href="https://doi.org/10.17882/91485">https://doi.org/10.17882/91485</a>
R/Vs L'Atalante and Maria S. Merian concatenated sections	Temperature/Salinity and Velocity	<a href="https://doi.org/10.17882/92071">https://doi.org/10.17882/92071</a>
UEA Gliders	Temperature/Salinity	<a href="https://doi.org/10.5285/c596cdd7-c709-461a-e053-6c86abc0c127">https://doi.org/10.5285/c596cdd7-c709-461a-e053-6c86abc0c127</a>
IFM and Kraken Gliders	Temperature/Salinity/Oxygen	<a href="https://observations.ipsl.fr/aeris/eurec4a/#/">https://observations.ipsl.fr/aeris/eurec4a/#/</a>
<b>Surface Only</b>		
<b>Platforms</b>	<b>Parameters</b>	<b>DOI/Access Data</b>
R/V L'Atalante TSG	Temperature/Salinity	<a href="https://observations.ipsl.fr/aeris/eurec4a/#/">https://observations.ipsl.fr/aeris/eurec4a/#/</a>
R/V Maria S. Merian TSG	Temperature/Salinity	<a href="https://doi.pangaea.de/10.1594/PANGAEA.951260">https://doi.pangaea.de/10.1594/PANGAEA.951260</a>
R/V Meteor TSG	Temperature/Salinity	<a href="https://doi.pangaea.de/10.1594/PANGAEA.951515">https://doi.pangaea.de/10.1594/PANGAEA.951515</a>
Saildrones	Temperature/Salinity and Velocity	<a href="https://doi.org/10.5067/SDRON-ATOM0">https://doi.org/10.5067/SDRON-ATOM0</a>
Argo Floats	Temperature/Salinity/Oxygen	<a href="https://dataselection.coriolis.eu.org/">https://dataselection.coriolis.eu.org/</a>
Surface Drifters	Temperature/Salinity	<a href="https://observations.ipsl.fr/aeris/eurec4a/#/">https://observations.ipsl.fr/aeris/eurec4a/#/</a>

**Table 1.** Table summarizing the DOIs and parameters measured by type of observation platform.

## 7 Conclusions

The oceanic instruments deployed during the EUREC<sup>4</sup>A-OA experiment provide a large set of observations characterized by different oceanic structures, including mesoscale eddies intensified at the surface or at depth, finer scale filaments, and salinity barrier layers. Nevertheless, the wide variety of devices at our disposal require precise pre- and post-cruise calibrations and cross validations, so the data can be used to its full potential. In this study, we aimed at describing all sensors and their measurements, the sources of errors, and the methods used to correct them. Then, we ranked them, taking into account how they were validated and how they can be related to one another. The adopted strategy and the complementarity of the different observations enable descriptions and quantification of such processes with unprecedented detail. This underlines the importance of deploying CTD stations, our only way to compare water parcels sampled at depth with sensor measurements by performing close-by profiles with other devices or attaching probes to the rosette. With that, we are able to, at best, correct the measure-



ments from other sensors, or at least, quantify their uncertainties.

We propose here a way of estimating the uncertainties by assessing the three main sources of variability between measurement on isopycnal levels or at the surface : background oceanic variability (lateral variability and internal wave field) and the sensor variability. The background oceanic variability is strongly depth dependent, thus for comparison we chose to compare profiles on isopycnal levels, only focusing on measurements performed below the mixing layer. Nevertheless, this method strongly depends on the number of observations and their calibrations and validations using water samples. It also underlines the importance of having synoptic profiles of the devices for comparison and hence, corrections. In the end, we make available a finalized dataset with calibrated and cross-validated thermohaline, chemical, and dynamical measurements, with their associated uncertainties after secondary QC.

*Author contributions.* Pierre L'Hégaret performed the secondary quality control and adjustments to the uCTD, MVP and Gliders measurements, their cross-calibration, and wrote this manuscript. Florian Schütte worked on the comparison of the CTD calibration methods from GEOMAR and IFREMER, and on the calibration of the uCTD profiles. Sabrina Speich, Gilles Reverdin, and Johannes Karstensen contributed to the manuscript writing and conceived of and led a major component of EUREC<sup>4</sup>A. Rémi Laxenaire, Gregory Foltz, Dongxiao Zhang made major contributions to the broader coordination and execution of scientific activities during and after the experiment. Corentin Subirade participated in the preparation and redaction of this manuscript. Karen J. Heywood, Elizabeth Siddle, and Callum Rollo deployed the UEA gliders and processed their data. The R/V Meteor CTD data were obtained and processed by Darek Baranowski. The R/V Meteor ADCP data were undertaken onboard by Callum Rollo, and subsequently processed by Tim Fischer. Rena Czeschel processed the ADCP data from the R/Vs Maria S. Merian. Michael Schlundt processed the TSG data from the R/Vs Maria S. Merian and Meteor. Gerd Krahnmann processed the CTD, uCTD, MVP, and glider (IFM03, 09, 12) data. Philippe Le Bot and Stéphane Leizour processed the CTD and uCTD data on board of the R/V L'Atalante. Caroline Le Bihan processed the CTD data from the R/V L'Atalante and performed its calibration.

*Competing interests.* No competing interests are present.

*Acknowledgements.* This research has been supported by the people and government of Barbados; by the European Research Council (ERC) advanced grant EUREC4A (grant agreement no. 694768) under the European Union's Horizon 2020 research and innovation program (H2020), with additional support from CNES (the French National Center for Space Studies) through the TOSCA SMOS-Ocean, TOEddies, and EUREC4A-OA proposals, the French national program LEFE INSU, IFREMER, the French research fleet, the French research infrastructures AERIS and ODATIS, IPSL, the EUREC4A-OA JPI Ocean and Climate program, the Chaire Chanel program of the Geosciences Department at ENS, Météo-France, by the Max Planck Society and its supporting members and by the German Research Foundation (DFG) and the German Federal Ministry of Education and Research (grant nos. GPF18-1-69 and GPF18-2-50). DBB was supported by the Poland's National Science Centre (grant no.UMO-2018/30/M/ST10/00674). We also acknowledge the mesoscale calculation server



<https://doi.org/10.5194/essd-2022-402>  
Preprint. Discussion started: 9 December 2022  
© Author(s) 2022. CC BY 4.0 License.



CICLAD <http://ciclad-web.ipsl.jussieu.fr> dedicated to Institut Pierre Simon Laplace modeling effort for technical and computational support. We also warmly thank the captain and crew of RVs Atalante, Maria S. Merian, Meteor and Ronald H. Brown. Gregory Foltz was supported by the CVP Program of NOAA's Climate Program Office, and by base funds to NOAA/AOML.

655



## References

- Argo, G.: Argo float data and metadata from global data assembly centre (Argo GDAC), Seanoe, 2000.
- Bacon, S., Culkin, F., Higgs, N., and Ridout, P.: IAPSO Standard Seawater: definition of the uncertainty in the calibration procedure, and stability of recent batches, *Journal of Atmospheric and Oceanic Technology*, 24, 1785–1799, 2007.
- 660 Bourras, D., Branger, H., Reverdin, G., Marié, L., Cambra, R., Baggio, L., Caudoux, C., Caudal, G., Morisset, S., Geyskens, N., et al.: A new platform for the determination of air–sea fluxes (ocarina): Overview and first results, *Journal of Atmospheric and Oceanic Technology*, 31, 1043–1062, 2014.
- Branellec, P., Le Bihan, C., and Speich, S.: EUREC4A 2020. CTD-O2 Data report, 2020.
- Eaton, B., Gregory, J., Drach, B., Taylor, K., Hankin, S., Caron, J., Signell, R., Bentley, P., Rappa, G., Höck, H., et al.: NetCDF Climate and  
665 Forecast (CF) metadata conventions, 2003.
- Firing, E., Hummon, J. M., and Chereskin, T. K.: Improving the quality and accessibility of current profile measurements in the Southern Ocean, *Oceanography*, 2012.
- Fratantoni, D. M., Johns, W. E., and Townsend, T. L.: Rings of the North Brazil Current: Their structure and behavior inferred from observations and a numerical simulation, *Journal of Geophysical Research: Oceans*, 100, 10 633–10 654, 1995.
- 670 Gentemann, C., Vazquez, J., and Tang, W.: 2020 Atomic Saildrone Cruise Report, <https://doi.org/https://doi.org/10.5281/zenodo.5201863>, 2020.
- Gouretski, V. and Jancke, K.: Systematic errors as the cause for an apparent deep water property variability: global analysis of the WOCE and historical hydrographic data, *Progress in Oceanography*, 48, 337–402, 2000.
- Hood, E., Sabine, C., and Sloyan, B.: The GO-SHIP repeat hydrography manual: A collection of expert reports and guidelines, IOCCP Rep,  
675 14, 2010.
- Karstensen, J., Lavik, G., Kopp, A., Mehlmann, M., Boeck, T., Ribbe, J., Guettler, J., Nordsiek, F., Philippi, M., Bodenschatz, E., et al.: EUREC4A Campaign, Cruise No. MSM89, 17 January–20 February 2020, Bridgetown Barbados–Bridgetown Barbados, The ocean mesoscale component in the EUREC4A++ field study, MARIA S. MERIAN-Berichte, 2020.
- Larson, N. and Pedersen, A.: Temperature measurements in flowing water: Viscous heating of sensor tips, in: Proc. of the First IGHEM  
680 Meeting, Montreal, QC, Canada, International Group for Hydraulic Efficiency Measurement.[Available online at [http://www.seabird.com/technical\\_references/viscous.htm](http://www.seabird.com/technical_references/viscous.htm)]. 1996.
- Laxenaire, R., Speich, S., Blanke, B., Chaigneau, A., Pegliasco, C., and Stegner, A.: Anticyclonic eddies connecting the western boundaries of Indian and Atlantic Oceans, *Journal of Geophysical Research: Oceans*, 123, 7651–7677, 2018.
- Le Bot, P., Kermabon, C., Lherminier, P., and Gaillard, F.: CASCADE V6. 1: Logiciel de validation et de visualisation des mesures ADCP  
685 de coque, 2011.
- Liblik, T., Karstensen, J., Testor, P., Alenius, P., Hayes, D., Ruiz, S., Heywood, K., Pouliquen, S., Mortier, L., and Mauri, E.: Potential for an underwater glider component as part of the Global Ocean Observing System, *Methods in Oceanography*, 17, 50–82, 2016.
- Lueck, R. G.: Thermal inertia of conductivity cells: Theory, *Journal of Atmospheric and Oceanic Technology*, 7, 741–755, 1990.
- Lueck, R. G. and Picklo, J. J.: Thermal inertia of conductivity cells: Observations with a Sea-Bird cell, *Journal of Atmospheric and Oceanic  
690 Technology*, 7, 756–768, 1990.
- Mensah, V., Roquet, F., Siegelman-Charbit, L., Picard, B., Pauthenet, E., and Guinet, C.: A correction for the thermal mass-induced errors of CTD tags mounted on marine mammals, *Journal of atmospheric and oceanic technology*, 35, 1237–1252, 2018.



- Mohr, W., Kinne, S., Baier, K., Baranowski, D., Chilinski, M., Gollop, J., de Groot, G., Grosz, R., Helfer, K., Ibáñez-Landeta, A., Kalesse, H., Kidane, A., Los, S., Makuch, P., Meyer, M., Morfa-Avalos, Y., Neuberger, A., Nowak, J., Raeke, A., Rollo, C., Röttenbacher, J., Sandiford, S., Schirmacher, I., Schlenczek, O., Schröder, M., Siddle, E., Szkolka, W., Ubele, A. A., von Arx, J., and Worbes, L.: EUREC4A Campaign, Cruise No. M161, 17 Jan 2020 - 03 Mar 2020, Bridgetown *Barbados* - Ponta Delgada *Portugal*, METEOR-Berichte, [https://doi.org/10.2312/cr\\_m161](https://doi.org/10.2312/cr_m161), 2020.
- Otosaka, S., Ueki, I., Sasano, D., Kumamoto, Y., Obata, H., Fukuda, H., Nishibe, Y., Maki, H., Goto, K., Ono, T., et al.: Guideline of ocean observations, Volumes 1-10, 2020.
- Perkin, R., Lewis, E., et al.: Design of CTD observational programmes in relation to sensor time constants and sampling frequencies, 1982.
- Quinn, P. K., Thompson, E. J., Coffman, D. J., Baidar, S., Bariteau, L., Bates, T. S., Bigorre, S., Brewer, A., De Boer, G., De Szoeko, S. P., et al.: Measurements from the RV Ronald H. Brown and related platforms as part of the Atlantic Tradewind Ocean-Atmosphere Mesoscale Interaction Campaign (ATOMIC), *Earth System Science Data*, 13, 1759–1790, 2021.
- Reverdin, G., Olivier, L., Foltz, G., Speich, S., Karstensen, J., Horstmann, J., Zhang, D., Laxenaire, R., Carton, X., Branger, H., et al.: Formation and evolution of a freshwater plume in the northwestern tropical Atlantic in February 2020, *Journal of Geophysical Research: Oceans*, 126, e2020JC016981, 2021.
- Rudnick, D. L. and Klinke, J.: The underway conductivity–temperature–depth instrument, *Journal of Atmospheric and Oceanic Technology*, 24, 1910–1923, 2007.
- Sloyan, B. M., Wanninkhof, R., Kramp, M., Johnson, G. C., Talley, L. D., Tanhua, T., McDonagh, E., Cusack, C., O’rourke, E., McGovern, E., et al.: The global ocean ship-based hydrographic investigations program (GO-SHIP): a platform for integrated multidisciplinary ocean science, *Frontiers in Marine Science*, 6, 445, 2019.
- Speich, S. et al.: EUREC4A-OA. Cruise Report. 19 January–19 February 2020. Vessel: L’ATALANTE, 2021.
- Stevens, B., Bony, S., Farrell, D., Ament, F., Blyth, A., Fairall, C., Karstensen, J., Quinn, P. K., Speich, S., Acquistapace, C., et al.: EURECA, *Earth System Science Data*, 13, 4067–4119, 2021.
- Tanhua, T., Van Heuven, S., Key, R. M., Velo, A., Olsen, A., and Schirnack, C.: Quality control procedures and methods of the CARINA database, *Earth System Science Data*, 2, 35–49, 2010.
- Thurnherr, A., Visbeck, M., Firing, E., King, B., Hummon, J., Krahnmann, G., and Huber, B.: A manual for acquiring lowered Doppler current profiler data, 2010.
- Ullman, D. S. and Hebert, D.: Processing of underway CTD data, *Journal of Atmospheric and Oceanic Technology*, 31, 984–998, 2014.
- Winkler, L. W.: The determination of dissolved oxygen in water, *Berlin DeutChem Gas*, 21, 2843–2855, 1888.
- Wong, A. P., Johnson, G. C., and Owens, W. B.: Delayed-mode calibration of autonomous CTD profiling float salinity data by  $\theta$ - $S$  climatology, *Journal of Atmospheric and Oceanic Technology*, 20, 308–318, 2003.

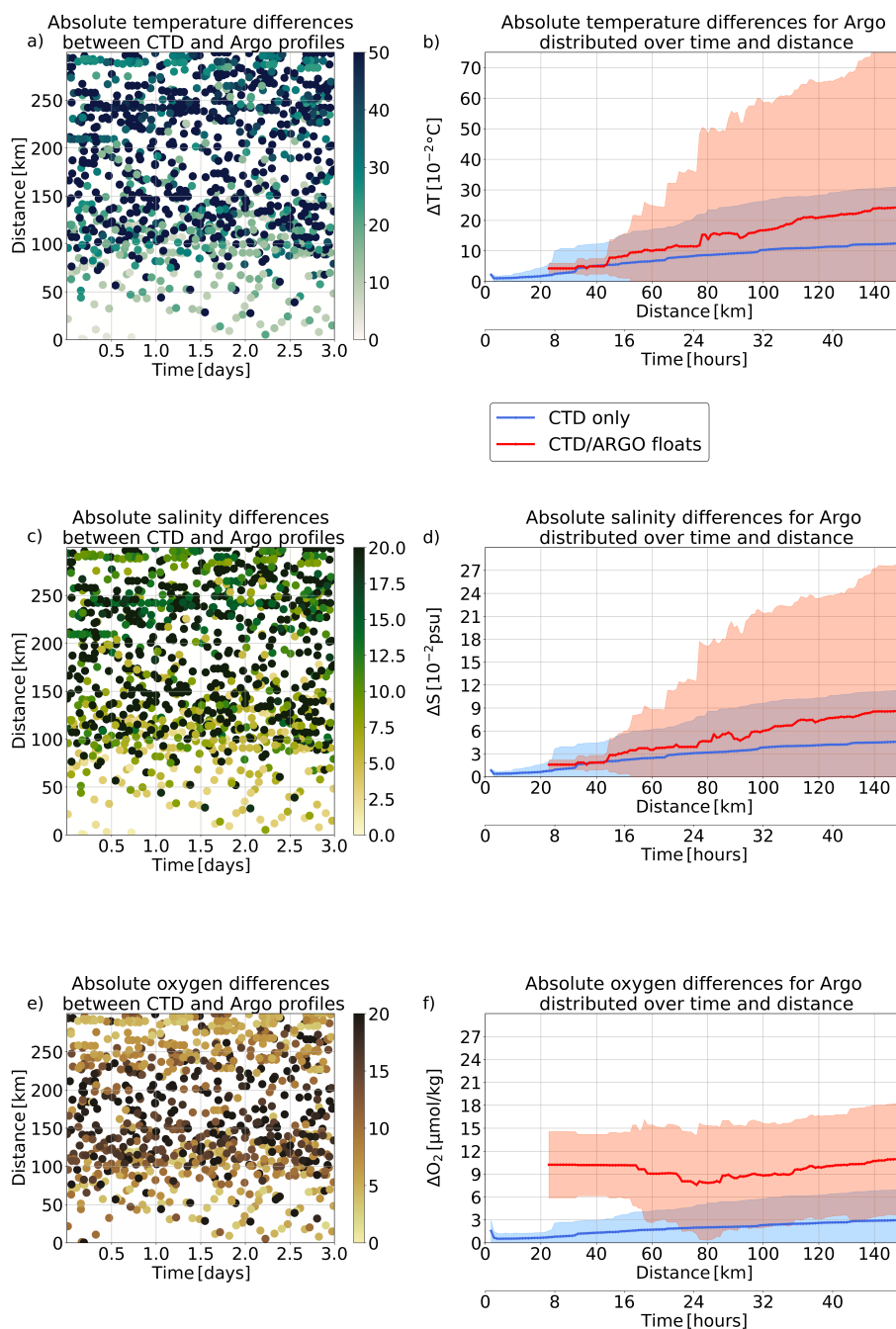


**Figure 18.** a) Absolute temperature differences between CTD/Argo floats pairs of profiles on isopycnal levels and averaged vertically distributed in time and distance. Each pair is composed of one CTD and one Argo float profiles. b) Temperature differences as a function of time and distance for pairs of profiles. In blue for pairs of CTD only profiles, in red for pairs composed of one CTD and one Argo float profiles. The middle line of panels is the same as above, but for absolute salinity differences. The bottom line of panels correspond to absolute oxygen differences.

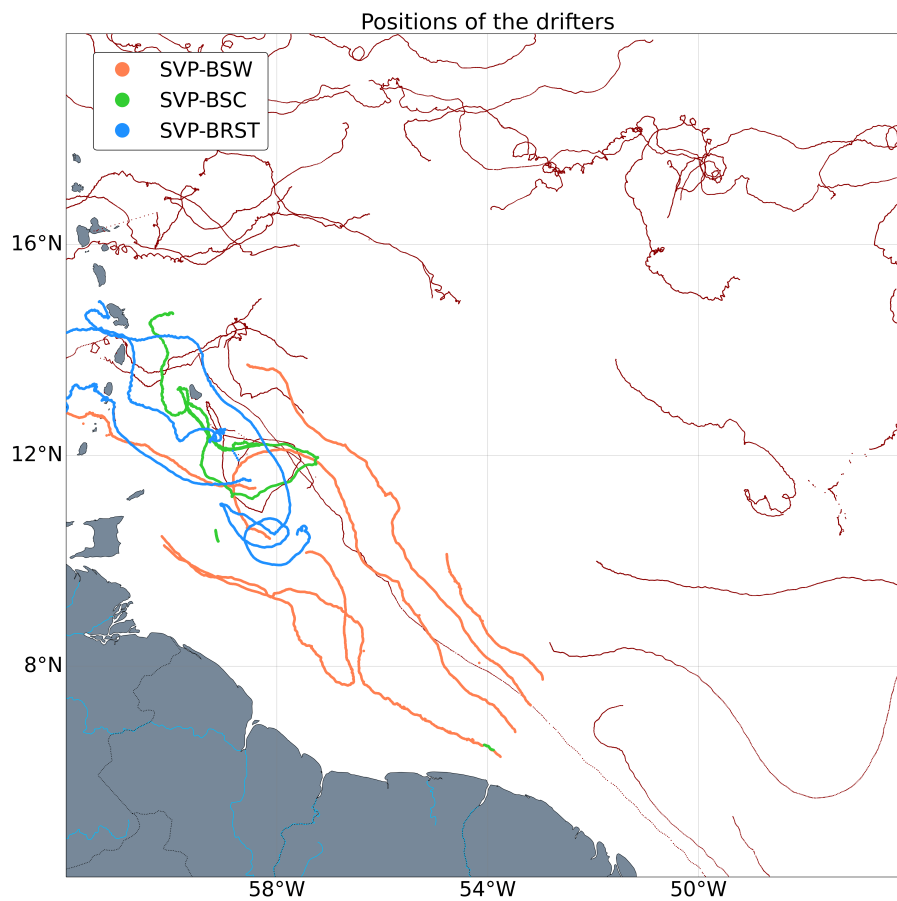


**Figure 19.** Map of the drifters positions from December 2019 to May 2020. Thick colored lines display the drifters that have been deployed from the R/V L'Atalante, while thin red lines shows the other drifters observed in the region during the same period.

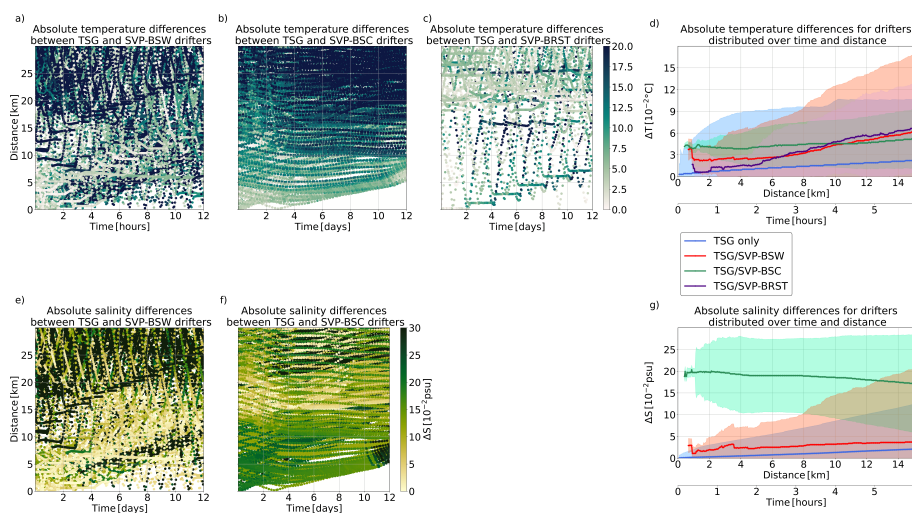


**Figure 20.** a), b), and c) Absolute temperature differences between TSG/drifters pairs of measurements distributed in time and distance. Each pair is composed of one R/V's TSG measurement and a drifter's one. Respectively a), b), and c), correspond to the SVP-BSW, SVP-BSC, and SVP-BRST drifters. d) Temperature differences as a function of time and distance for a pair of surface measurements. In blue for pairs of CTD only profiles, in red for pairs composed of one TSG and one SVP-BSW measurements, in green for pairs composed of one TSG and one SVP-BSC measurements, and in purple for pairs composed of one TSG and one SVP-BRST measurements. e) to g), same as the above line, but for absolute salinity differences without the SVP-BRST drifters.

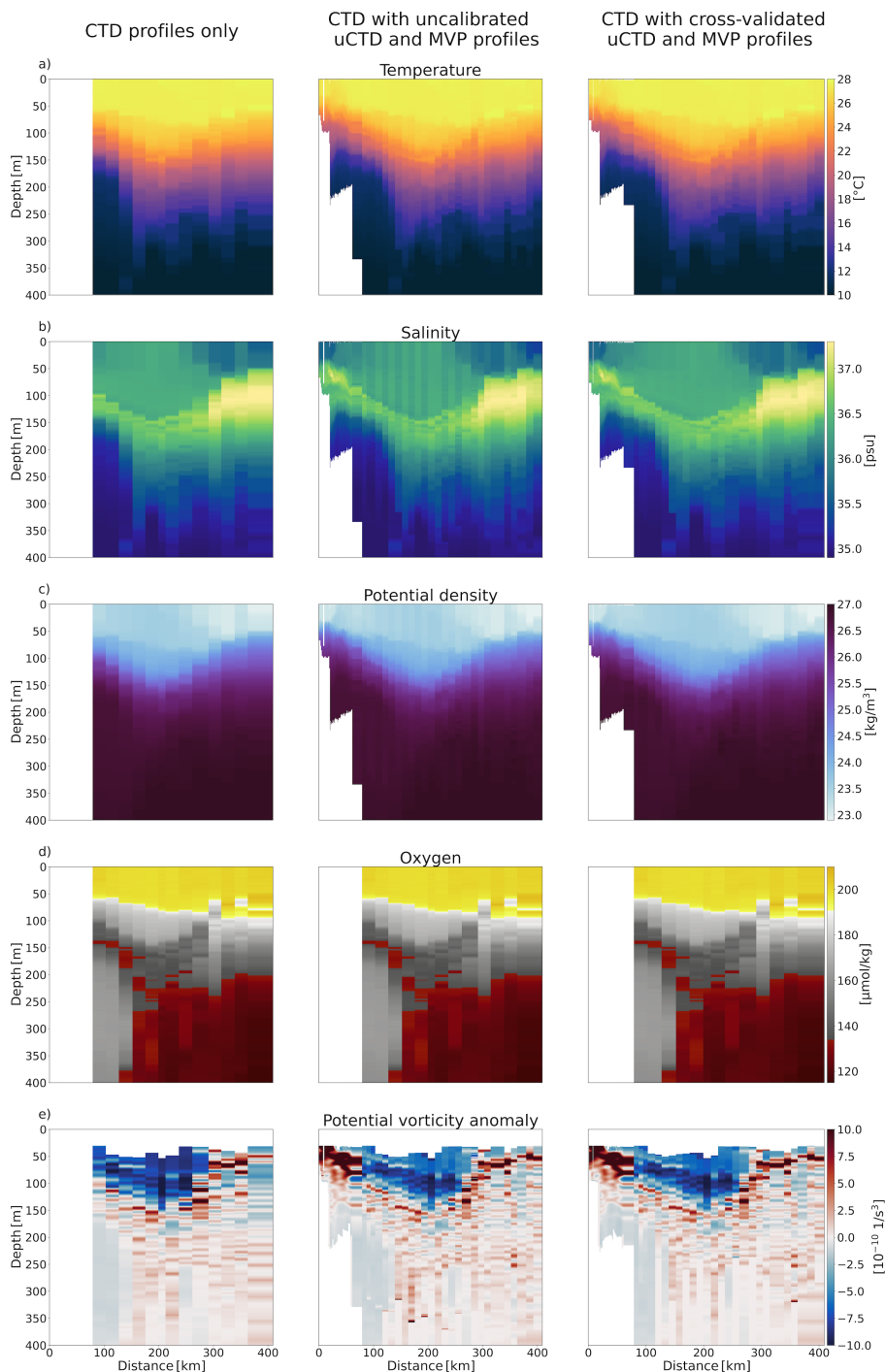


**Figure 21.** Vertical sections of thermohaline and dynamic characteristics performed by the R/V L'Atalante. The first column shows the section with only the CTD profiles, on the second column the uncalibrated profiles of MVP and uCTD are added, the third column is the same but for calibrated profiles. a) is for temperature, b) for salinity, c) for potential density, d) for oxygen (only CTD profiles measured oxygen), and e) for Ertel Potential Vorticity based on the ADCP measurements (not shown).